

Peronophythora litchii RXLR effector *P. litchii* avirulence homolog 202 destabilizes a host ethylene biosynthesis enzyme

Peng Li ,¹ Wen Li ,¹ Xiaofan Zhou ,² Junjian Situ ,¹ Lizhu Xie ,¹ Pinggen Xi ,¹ Bo Yang ,³ Guanghui Kong ,^{1,*} and Zide Jiang ,^{1,*}

¹ Guangdong Key Laboratory of Microbial Signals and Disease Control/Department of Plant Pathology, College of Plant Protection, South China Agricultural University, Guangzhou 510642, China

² Integrative Microbiology Research Centre, South China Agricultural University, Guangzhou 510642, China

³ College of Grassland Science/Department of Plant Pathology, College of Plant Protection, Nanjing Agricultural University, Nanjing 210095, China

*Author for correspondence: gkong@scau.edu.cn (G.K.), zdjiang@scau.edu.cn (Z.J.)

The author responsible for distribution of materials integral to the findings presented in this article in accordance with the policy described in the Instructions for Authors (<https://academic.oup.com/plphys/pages/General-Instructions>) is Zide Jiang (zdjiang@scau.edu.cn).

Abstract

Oomycete pathogens can secrete hundreds of effectors into plant cells to interfere with the plant immune system during infection. Here, we identified a Arg-X-Leu-Arg (RXLR) effector protein from the most destructive pathogen of litchi (*Litchi chinensis* Sonn.), *Peronophythora litchii*, and named it *P. litchii* avirulence homolog 202 (PIAvh202). PIAvh202 could suppress cell death triggered by infestin 1 or avirulence protein 3a/resistance protein 3a in *Nicotiana benthamiana* and was essential for *P. litchii* virulence. In addition, PIAvh202 suppressed plant immune responses and promoted the susceptibility of *N. benthamiana* to *Phytophthora capsici*. Further research revealed that PIAvh202 could suppress ethylene (ET) production by targeting and destabilizing plant S-adenosyl-L-methionine synthetase (SAMS), a key enzyme in the ET biosynthesis pathway, in a 26S proteasome-dependent manner without affecting its expression. Transient expression of LcSAMS3 induced ET production and enhanced plant resistance, whereas inhibition of ET biosynthesis promoted *P. litchii* infection, supporting that litchi SAMS (LcSAMS) and ET positively regulate litchi immunity toward *P. litchii*. Overall, these findings highlight that SAMS can be targeted by the oomycete RXLR effector to manipulate ET-mediated plant immunity.

Introduction

Both pathogens and plants have evolved diverse pathways to counter each other for more beneficial growing conditions in the long process of coevolution. To resist the invasion of pathogens, plants have 2 layers of defense systems. First, certain conserved pathogen-associated molecular patterns (PAMPs) can be recognized by plant cell surface pattern-recognition receptors to trigger basal defense responses, known as PAMP-triggered immunity (PTI) (Jones and Dangl

2006; DeFalco and Zipfel 2021). For instance, bacterial flagellin, elongation factor Tu, and *Phytophthora infestans* elicitin infestin 1 (INF1) are typical PAMPs which are recognized by *Arabidopsis* (*Arabidopsis thaliana*) FLAGELLIN-SENSING 2 (FLS2), EF-Tu RECEPTOR, and potato RECEPTOR-LIKE PROTEIN 85, respectively, leading to promoted plant resistance (Gómez-Gómez and Boller 2000; Zipfel et al. 2006; Du et al. 2015). However, a variety of pathogens can secrete virulence-related molecules, such as effectors, to suppress plant PTI for successful infection (Jwa and Hwang 2017;

Naveed et al. 2020; Teixeira et al. 2021). As a response, plants initiate the second layer of defense with the activation of resistance proteins (R proteins). These R proteins can specifically recognize pathogen effectors directly or indirectly to cause a cascade of downstream immune responses; this process is named effector-triggered immunity (ETI) (Yuan et al. 2021a, b). For example, the avirulence protein AVR3a^{K80I103} from *Ph. infestans* is specifically recognized by potato resistance protein R3a to trigger ETI-mediated cell death (Armstrong et al. 2005). *Pseudomonas syringae* effector AvrRpt2 indirectly activates R protein RPS2 by eliminating *Arabidopsis* protein RIN4, which induces a series of ETI responses (Axtell and Staskawicz 2003). Although PTI and ETI are initiated by diverse mechanisms, they both can result in reactive oxygen species (ROS) accumulation and hypersensitive response (HR), a form of programmed cell death (PCD) that can restrict pathogen proliferation (Adachi et al. 2015; Zebell and Dong 2015; Li et al. 2019).

Oomycetes comprise numerous destructive plant pathogens such as *Ph. infestans*, *Ph. sojae*, and *Peronophythora litchii*, which are great threats to economic crops (Kamoun et al. 2015). Thus, understanding the pathogenic mechanism is important to restrict the invasion of pathogens for higher crop yields. Oomycetes secrete numerous effectors into plant cells to interfere with the plant immune system, among which RXLR effectors have a substantial contribution to pathogen virulence (Anderson et al. 2015). The RXLR effectors exhibit sequence polymorphisms in general; however, they possess 2 highly conserved motifs, termed RXLR (Arg-X-Leu-Arg; X is any amino acid) and dEER (Asp-Glu-Glu-Arg; Asp is less conserved than other 3 amino acids), following the N-terminal signal peptide (SP) (Wawra et al. 2012). Previous reports have shown that the RXLR motif is involved in plant cell entry (Whisson et al. 2007; Kale et al. 2010; Kale and Tyler 2011). RXLR effectors have various functions in plant-pathogen interactions, including both eliciting and suppressing cell death, under different circumstances. For example, AVR2 and Pi17316 from *Ph. infestans* could suppress INF1-triggered cell death (ICD) in *N. benthamiana*, depending on CIB1/HBI1-like1 and VASCULAR HIGHWAY1-interacting kinase, respectively (Turnbull et al. 2017; Murphy et al. 2018). Avr1b of *Ph. sojae* could suppress BAX-triggered cell death (Dou et al. 2008). On the other hand, *Ph. sojae* Avh241 and *Ph. capsici* RXLR207 could trigger cell death in *N. benthamiana* (Yu et al. 2012; Li et al. 2019). Large-scale screening assays of *Ph. sojae*, *Hyaloperonospora arabidopsis*, and *Plasmopara viticola* suggest that most RXLR effectors can suppress cell death triggered by several elicitors in *N. benthamiana*, whereas a few RXLR effectors trigger cell death (Fabro et al. 2011; Wang et al. 2011; Liu et al. 2018). These data support a hypothesis that most RXLR effectors secreted from pathogens mainly aim at suppressing the host immune system for infection. Thus, the study of effector-mediated PTI or ETI suppression is very valuable to reveal the mechanism of plant-pathogen interactions.

Salicylic acid (SA), jasmonic acid (JA), and ET are 3 major phytohormones in plant defense responses (Casteel et al. 2015). In

plants, the biosynthesis of ET begins with the conversion of L-methionine and ATP into S-adenosyl-L-methionine (SAM), catalyzed by S-adenosyl-L-methionine synthetase (SAMS) (EC 2.5.1.6). SAM is then converted to 1-aminocyclopropane-1-carboxylic acid (ACC) and methylthioadenosine by 1-aminocyclopropane-1-carboxylate synthase. ACC can be oxidized by ACC oxidases to produce ET (Park et al. 2021). Because SAM acts as a precursor of ET and polyamines, SAMS is important for ET production. Previous studies have showed that SAMS is involved in the regulation of plant resistance to viruses (Zhao et al. 2017; Ismayil et al. 2018). However, the role of SAMS in plant-pathogenic oomycete interactions remains unknown.

In our previous research, we predicted 245 RXLR effectors in *Pe. litchii* (Ye et al. 2016); however, their function in immune suppression is not fully understood. In this study, we found 4 *Pe. litchii* RXLR effectors, PIAvh42, PIAvh202, PIAvh208, and PIAvh222, that could suppress ICD, based on large-scale screening in *N. benthamiana*. Among them, PIAvh202 had a strong ability to suppress cell death triggered by INF1 or avirulence protein 3a/receptor protein 3a (Avr3a/R3a) and was required for *Pe. litchii* virulence. Therefore, we focused our investigation on PIAvh202 and found that PIAvh202 suppressed plant innate immune responses, including suppressing immune maker gene expression and ROS accumulation. In addition, we found that PIAvh202 could interact with *N. benthamiana* NbSAMS proteins, as well as the SAMS homologs in litchi, designated as litchi SAMS (LcSAMS), via its roles in virulence region IR2 (internal repeat). Moreover, PIAvh202 could not promote *Ph. capsici* infection in the absence of IR2 or in NbSAMS-silenced *N. benthamiana*, suggesting that PIAvh202 exerts its virulence by targeting SAMS. Furthermore, interacting with PIAvh202 could result in LcSAMSs degradation in vivo and semi-in vitro. In summary, our results reveal a mechanism wherein the RXLR effector PIAvh202 can destabilize plant SAMS via 26S proteasome to suppress ET-mediated plant immunity.

Results

PIAvh202 can suppress leaf cell death of *N. benthamiana* triggered by INF1 or Avr3a/R3a

PCD or HR is an important characteristic of PTI and ETI, and a number of effectors have been confirmed to suppress plant PCD or HR to disrupt PTI or ETI (Abramovitch et al. 2003; Liu et al. 2011; Dutra et al. 2020). In this study, each of 48 RXLR effectors of *Pe. litchii* without SP was transiently expressed in *N. benthamiana* leaves by *Agrobacterium tumefaciens* infiltration to test whether they could suppress ICD (Supplemental Table S1). INF1 was transiently expressed in the same infiltration region after 24 h. Eventually, we found that INF1 could not trigger cell death in *N. benthamiana* leaves when PIAvh42, PIAvh202, PIAvh208 or PIAvh222 was expressed individually. Meanwhile, the expression of red fluorescence protein (RFP) control in leaves did not suppress the cell death triggered by INF1 (Fig. 1, A and B). This result suggested that

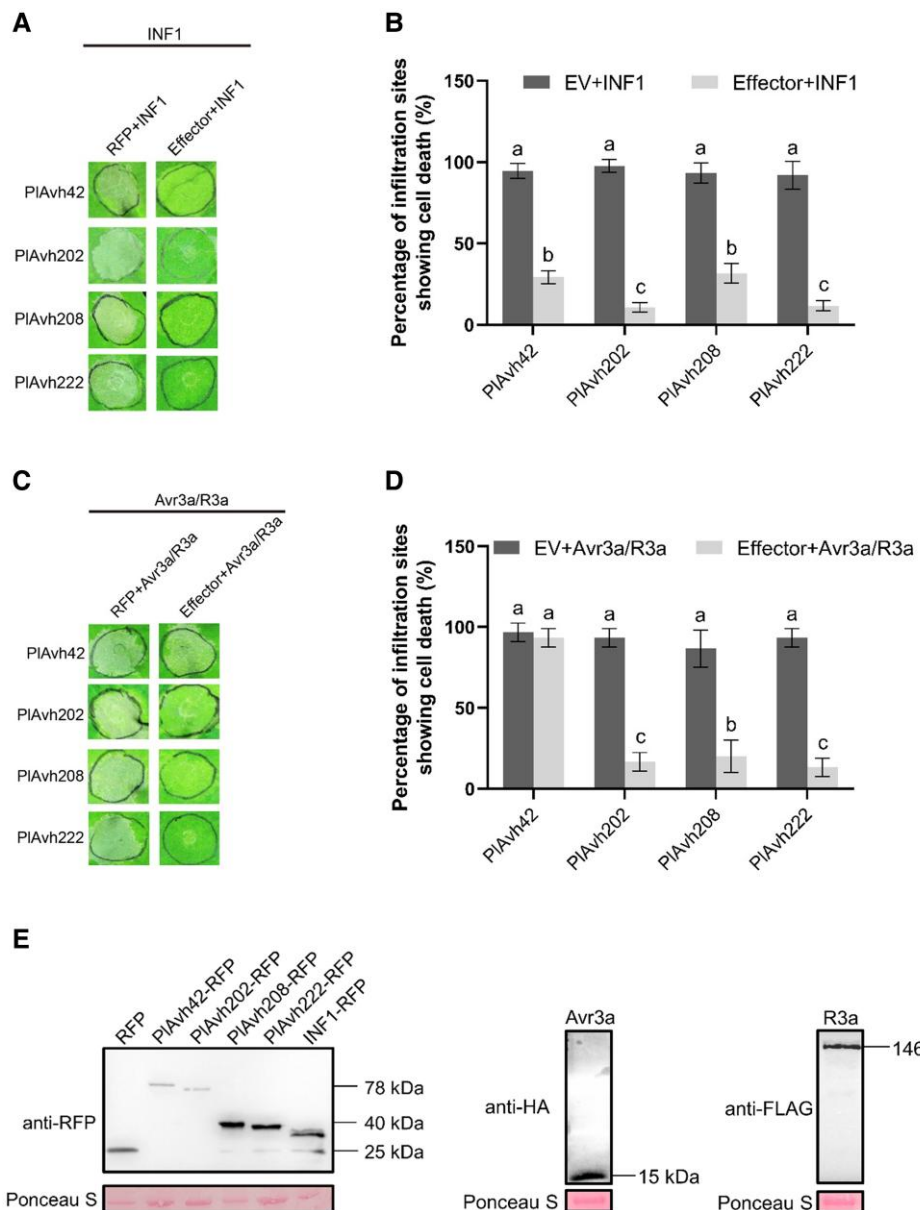


Figure 1. *Peronophythora litchii* RXLR effectors suppress cell death triggered by INF1 or Avr3a/R3a in *N. benthamiana*. **A, C**) Partial tissue responses to INF1 **A**) or Avr3a/R3a **C**) in the presence of *Pe. litchii* RXLR effectors. PIAvh202, PIAvh208, and PIAvh222 suppressed cell death triggered by INF1 or Avr3a/R3a; PIAvh42 only suppressed cell death triggered by INF1. Effecter-encoding genes were transiently expressed in *N. benthamiana* leaves by agroinfiltration, and then INF1 or Avr3a/R3a was transiently expressed in the indicated regions 24 h later. RFP was used as control. Photographs were taken at 3 days post-agroinfiltration (dpa). **B, D**) The percentage of cell death sites. The cell death triggered by INF1 **B**) and Avr3a/R3a **D**) were scored from effector-expressing sites. Different letters represent significant differences using the 1-way ANOVA test followed by Tukey's honestly significant difference (HSD) test ($P < 0.05$). Data are the means \pm SD of 3 independent biological replicates ($n \geq 5$ leaves). **E**) Immunoblot analysis. All proteins tested in the assay were confirmed using western blot, and total protein was stained by Ponceau S.

these 4 effectors, namely PIAvh42, PIAvh202, PIAvh208, and PIAvh222, could suppress ICD.

Next, we examined whether these 4 effectors were able to suppress cell death triggered by Avr3a/R3a in *N. benthamiana* leaves. The experiment result showed that 3 of these 4 RXLR effectors, PIAvh202, PIAvh208 and PIAvh222, could also suppress leaf cell death triggered by Avr3a/R3a, whereas PIAvh42 could not (Fig. 1, C and D). Protein expression of 4

tested effectors, INF1, and Avr3a/R3a were verified by western blot (Fig. 1E). Overall, these results indicated that PIAvh202, PIAvh208, and PIAvh222 could suppress plant cell death mediated by INF1 or Avr3a/R3a, while PIAvh42 only suppressed ICD. Given that PIAvh202 showed the strongest inhibitory effect on *N. benthamiana* leaf cell death among the 4 tested effectors, we selected PIAvh202 for further investigation.

PIAvh202 is critical for *Pe. litchii* virulence

To investigate the role of PIAvh202 in the virulence of *Pe. litchii*, we examined the expression pattern of PIAvh202 using reverse transcription quantitative PCR (RT-qPCR). The result showed that PIAvh202 was substantially up-regulated in zoospores and at 1.5, 3, 6 h post-inoculation (hpi) compared with the mycelial stage and that the highest expression level occurred in the zoospore stage (more than 1,800-fold) (Supplemental Fig. S1). This result suggested that PIAvh202 is highly expressed during early infection stages of *Pe. litchii* and indicated that PIAvh202 may contribute to the virulence of *Pe. litchii*.

To further explore the contribution of PIAvh202 to *Pe. litchii* virulence, we deleted the PIAvh202 gene in *Pe. litchii* by CRISPR/Cas9 technology (Fang et al. 2017) (Fig. 2A and Supplemental Fig. S2A). Three transformants (T7, T55, T95) were verified as successful PIAvh202 deletion mutants, based on PCR amplification and Sanger sequencing (Fig. 2B, Supplemental Fig. S2B). A transformant that failed to delete PIAvh202 was selected as control (CK). We next evaluated the virulence of these 3 PIAvh202 deletion mutants by inoculating their zoospores on litchi leaves, and the result showed that loss of the PIAvh202 gene caused reduced virulence, as smaller lesions were formed, compared to those caused by wild-type (WT) or CK inoculation (Fig. 2, C and D). This result suggested that PIAvh202 was required for the full virulence of *Pe. litchii*.

In addition, we also measured mycelial growth rates and found no statistically significant difference among WT, CK,

T7, T55, and T95 in their colony diameters (Supplemental Fig. S2, C and D), indicating that PIAvh202 deletion did not impact the mycelial growth of *Pe. litchii*.

PIAvh202 suppresses *N. benthamiana* immune responses induced by INF1 and promoted pathogen infection

Because of the ability of PIAvh202 to suppress PCD induced by INF1 in *N. benthamiana* leaves, we further explored its effect on the plant immune system. We evaluated the relative expression levels of marker genes related to SA, JA, ET, and ROS accumulation, including PR1/2 (pathogenesis-related protein 1/2), LOX (lipoxygenase), PDF1.2 (Plant defensin 1.2), RbohA, and RbohB (respiratory burst oxidase homologs) (Yoshioka et al. 2003; Pieterse et al. 2012; Yang et al. 2019; Ding and Ding 2020), using RT-qPCR. The result showed that the transient expression of PIAvh202 led to the reduced expression levels of NbPR1, NbPR2, NbLOX, NbRbohA, and NbRbohB at 24, 36, and 48 hpi. Although ET/JA pathway-related marker gene NbPDF1.2 was up-regulated at 24 hpi, its expression level was also down-regulated at 36 and 48 hpi (Fig. 3A). Together, these marker genes were suppressed by PIAvh202 at 36 and 48 hpi. Given that NbRbohA and NbRbohB are required for ROS accumulation in *N. benthamiana* to resist pathogens, it is speculated that PIAvh202 might reduce ROS production of *N. benthamiana*. To validate this hypothesis, we tested the ROS accumulation

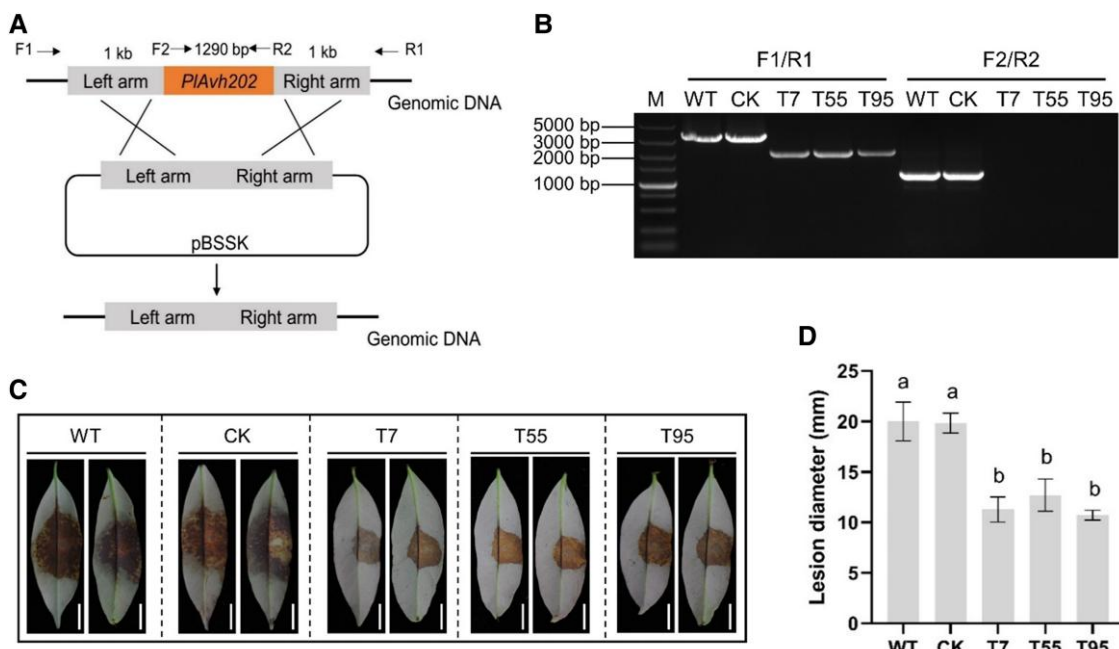


Figure 2. Deletion of PIAvh202 impairs the virulence of *Pe. litchii*. **A)** Schematic diagram of PIAvh202 deletion using CRISPR/Cas9. The primer pairs F1/R1 and F2/R2 used for PIAvh202 mutants screening are indicated by the horizontal arrows. **B)** PCR analysis of PIAvh202 mutants. Genomic DNA of WT, CK, T7, T55, and T95 was used for PCR assays using primer pairs F1/R1 and F2/R2, separately. **C)** Virulence assays of PIAvh202 mutants on litchi leaves. One hundred zoospores of WT, CK, T7, T55, and T95 were inoculated on the center of litchi leaves. Photographs were taken at 48 h post-inoculation (hpi). Bars = 1 cm. **D)** Lesion diameter of *Pe. litchii* infection at 48 hpi. Different letters represent significant differences using the 1-way ANOVA test followed by Tukey's honestly significant difference (HSD) test ($P < 0.05$). Data are the means \pm SD of 3 independent biological replicates ($n \geq 6$ leaves).

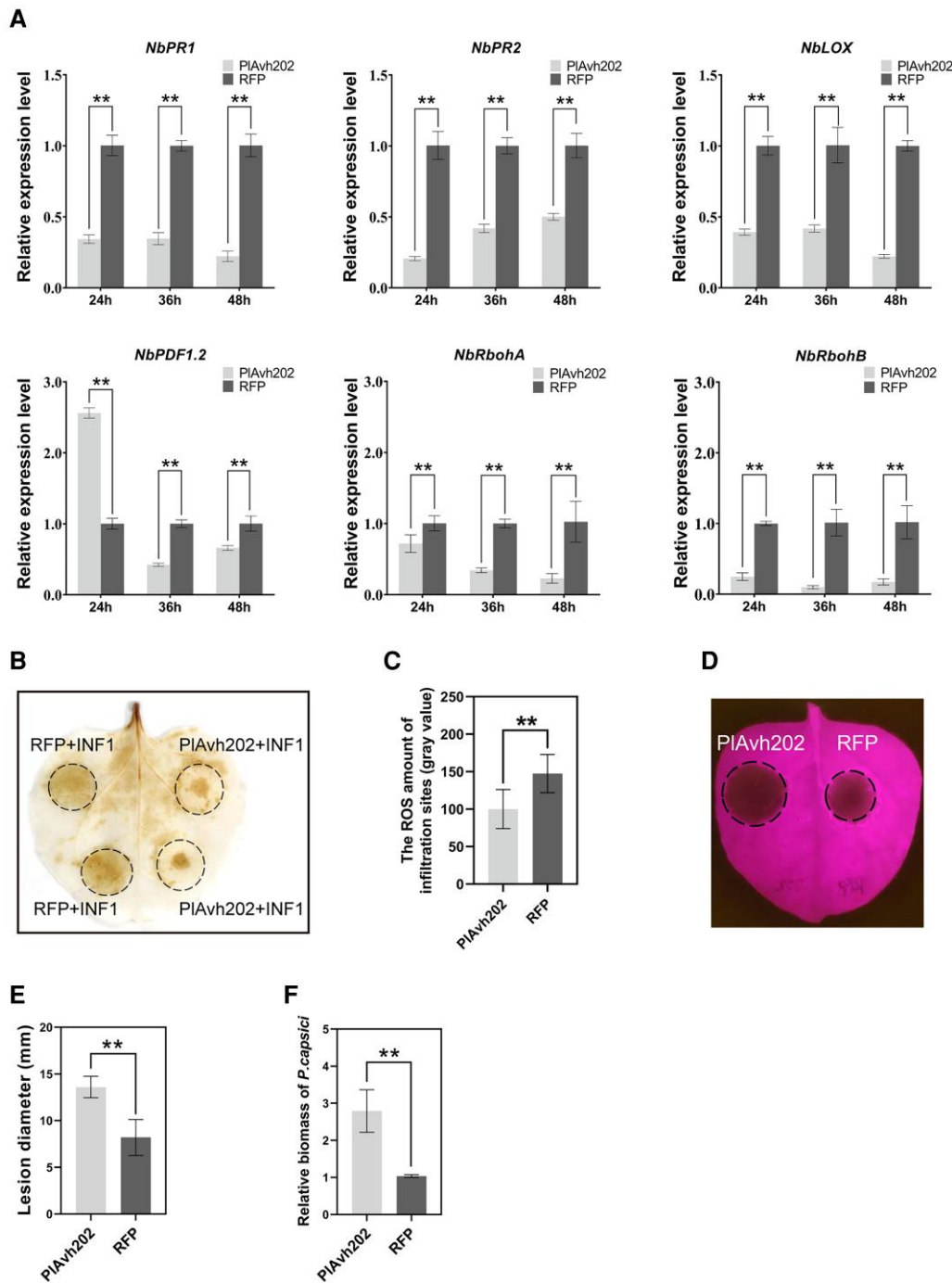


Figure 3. PlAvh202 suppresses INF1-triggered plant immune responses **A)** Expression profile analysis of immune marker genes. Relative expression levels of *NbPR1*, *NbPR2*, *NbLOX*, *NbPDF1.2*, *NbRbohA*, and *NbRbohB* induced by INF1 in the presence of PlAvh202 or RFP control were measured using RT-qPCR. The total RNA of *N. benthamiana* leaves was extracted at 24, 36, and 48 hpi. Data are the means \pm SD of 3 independent biological replicates (each sample of every experiment were from 3 leaves at each timepoint), asterisks represent significant differences ($**P < 0.01$, Student's t test). *NbEF1 α* was used as the internal reference. **B)** ROS accumulation in *N. benthamiana*. The leaves were stained using 1 mg/mL DAB at 36 h after agroinfiltration with Agrobacterium carrying PlAvh202, INF1, or RFP. The black circles indicate the inoculation region. The image was digitally extracted for comparison. **C)** The suppression levels of ROS accumulation. The ROS amount of infiltrated sites were represented by the mean of gray value, which is calculated using an Image J software. Data are the means \pm SD of 3 independent biological replicates ($n \geq 3$), asterisks represent significant differences ($**P < 0.01$, Student's t test). **D)** PlAvh202 promoted *Ph. capsici* infection in *N. benthamiana* leaves. *N. benthamiana* leaves were infiltrated with Agrobacterium carrying RFP or PlAvh202, and then the infiltrated leaves were inoculated with *Ph. capsici* at 24 h after infiltration. Photographs were taken under UV light at 36 hpi. Black circles indicate lesion areas. **E, F)** Lesion diameter **E)** and biomass **F)** of *Ph. capsici* in *N. benthamiana* leaves expressing PlAvh202 or RFP. Data are the means \pm SD of 3 independent biological replicates ($n \geq 3$), asterisks represent significant differences ($**P < 0.01$, Student's t test). *PcActin* and *NbEF1 α* were used for qPCR to analyze the biomass of *Ph. capsici*.

of *N. benthamiana* leaves using DAB staining after expressing PIAvh202 and INF1 successively. The brown area corresponding to ROS of PIAvh202-expressing leaves was significantly smaller than that of RFP (Fig. 3, B and C), suggesting PIAvh202 could attenuate INF1-triggered ROS accumulation in *N. benthamiana*. Thus, we conclude that PIAvh202 can suppress *N. benthamiana* immune responses induced by INF1.

In order to demonstrate whether overexpression of PhAvh202 increases plant susceptibility to pathogens, we inoculated *Ph. capsici* on the *N. benthamiana* leaves in which PIAvh202 or RFP was transiently expressed. The result showed that the lesion area was larger in the presence of PIAvh202 than that of RFP (Fig. 3, D and E). In addition, the biomass of *Ph. capsici* was also significantly higher in

PIAvh202-expressing leaves compared with RFP (Fig. 3F). These results suggested PIAvh202 could promote the infection of *Ph. capsici* in *N. benthamiana*.

A C-terminal internal repeat is required for PIAvh202-mediated ICD suppression

The analysis of amino acid sequence using SMART (<http://smart.embl-heidelberg.de/>) showed that PIAvh202 was composed of an N-terminal SP (1 to 23 aa), a typical RXLR-EER motif (24 to 49 aa), and 2 C-terminal internal repeat (IR) motifs (IR1, 67 to 130 aa and IR2, 273 to 338 aa). Therefore, we constructed 4 truncated constructs of PIAvh202 without the SP to identify the functional region of PIAvh202 (Fig. 4A). These 4 constructs (M1, M2, M3, and M4) were transiently

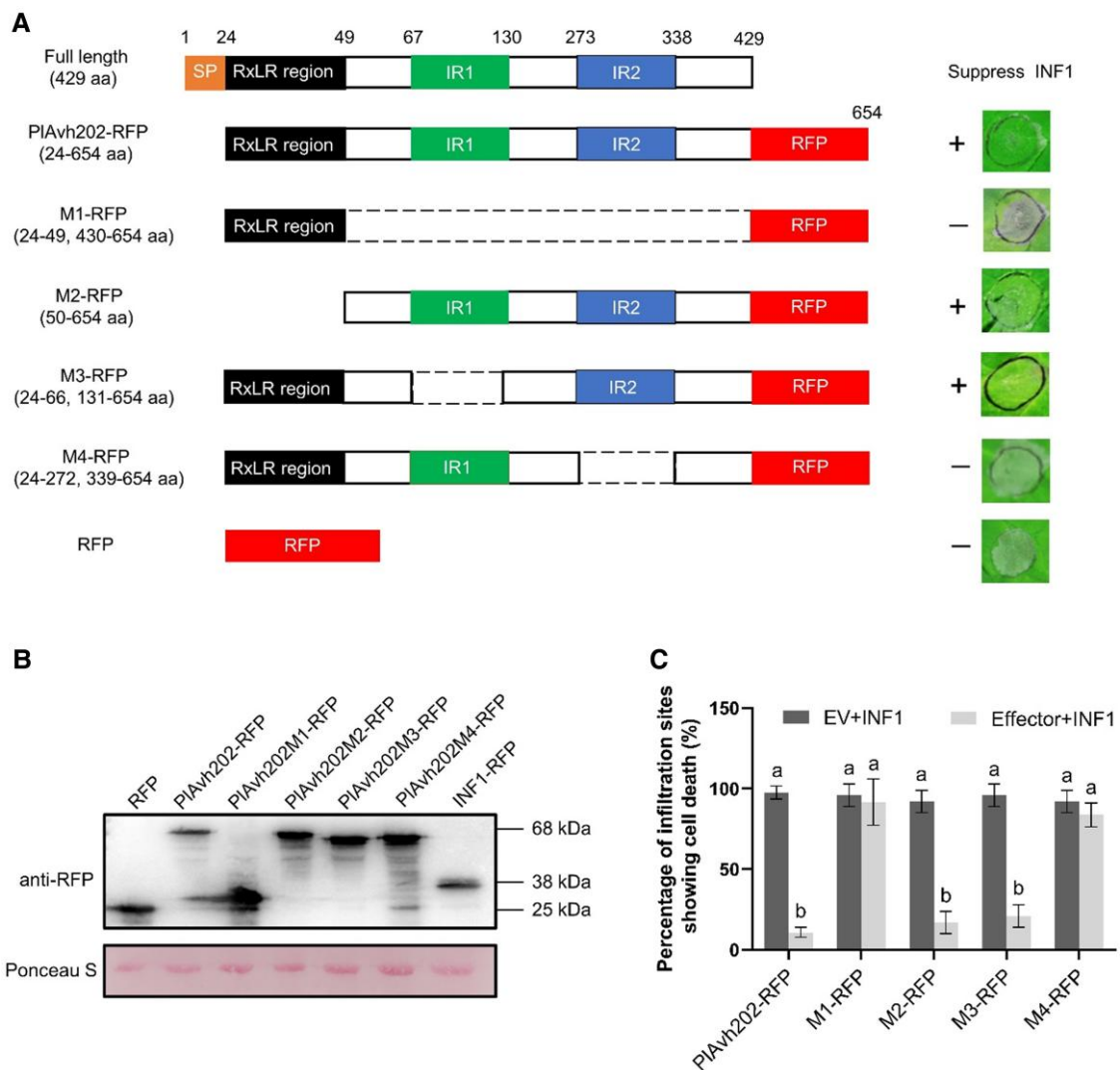


Figure 4. IR2 is required for PIAvh202 to suppress ICD. **A)** ICD suppression of PIAvh202 and its deletion mutants. Right panel is cell death symptoms in *N. benthamiana* leaves expressing PIAvh202 deletion mutants and INF1. Photographs were taken at 60 hpi, “-” represents the absence of ICD suppression, “+” represents ICD suppression. **B)** Immunoblot analysis. INF1, RFP, PIAvh202 and its deletion mutants were detected by western blot using anti-RFP antibody. Total protein was stained by Ponceau S. **C)** The percentage of cell death sites. The cell death triggered by INF1 was scored from PIAvh202 and its mutant-expressing sites. Different letters represent significant differences using the 1-way ANOVA test followed by Tukey's honestly significant difference (HSD) test ($P < 0.05$). Data are the means \pm SD of 3 independent biological replicates ($n \geq 3$ leaves).

expressed in *N. benthamiana*, as confirmed by western blotting (Fig. 4B). As shown in Fig. 4, A and C, the truncation M1 containing only the RXLR-EER region lost its ability to suppress ICD, demonstrating that the RXLR-EER motif could not suppress ICD. In contrast, the truncation M2, which does not contain the RXLR region, retained the ability to suppress ICD, suggesting that IR1 and IR2 might be critical for ICD suppression. To further investigate the contribution of IR1 and IR2, we individually deleted IR1 or IR2 (M3 or M4) and tested their ability of ICD suppression. INF1-induced *N. benthamiana* cell death was observed in the leaves expressing M4 but not M3 version of PIAvh202, suggesting that IR2 plays an essential role in ICD suppression.

PIAvh202 predominantly localizes to the cytoplasm

To determine the intracellular distribution of PIAvh202, PIAvh202-RFP was transiently coexpressed in *N. benthamiana* with free GFP (marking the nucleus and the cytoplasm) via agroinfiltration. PIAvh202-RFP was found at the periphery of cells and nucleus using laser confocal fluorescence microscopy (Fig. 5A), suggesting that PIAvh202 might be located at plasma membrane (PM), cytoplasm, endoplasmic reticulum (ER) or nuclear envelope. To further identify the specific subcellular location, PIAvh202 without SP was fused with an enhanced green fluorescent protein at its N-terminal and coexpressed with a PM marker AtPIP2A-RFP (Gonzalez et al. 2005) and an ER marker HDEL-mCherry (Fan et al. 2020), respectively. As shown in Fig. 5A, GFP-PIAvh202 did not colocalize with AtPIP2A-RFP or HDEL-mCherry in a cell, indicating that PIAvh202 may not localize at PM or ER. Furthermore, we extracted membrane and cytosolic proteins of PIAvh202-RFP and AtPIP2A-RFP which were individually expressed in *N. benthamiana*. Utilizing western blot, we could only detect PIAvh202-RFP in the cytosol fraction, while AtPIP2A-RFP was only detected in the membrane fraction (Fig. 5B). This result indicated that PIAvh202 localized to cytoplasm. Given that the subcellular localization of PIAvh202 was similar to ER proteins and we could not completely rule out the possibility that a few of PIAvh202 localized to the ER membrane using western blot. Therefore, we concluded that PIAvh202 predominantly localized to cytoplasm, may partially localized to ER.

In addition, we also examined the subcellular location of M1, M2, M3, and M4; the result showed that M2, M3, and M4 were coincident with PIAvh202, but M1 had an extra nuclear localization (Supplemental Fig. S3A). In order to clarify if the nuclear localization of PIAvh202 has an impact on ICD suppression, we fused a nuclear localization signal (NLS) or mutated NLS (nls) to the C terminus of GFP-PIAvh202. The expression of GFP-PIAvh202^{NLS} and PIAvh202^{nls} proteins were confirmed by western blot (Supplemental Fig. S3B). Confocal imaging showed that GFP-PIAvh202^{NLS} was exclusively localized in nuclei, while GFP-PIAvh202^{nls} had the same subcellular localization pattern as GFP-PIAvh202 (Fig. 5A). Moreover, PIAvh202^{nls} could suppress ICD as PIAvh202 in *N. benthamiana*, but PIAvh202^{NLS} lost the ability of ICD suppression (Fig. 5, C and D). These results suggested

that the nuclear localization of PIAvh202 could lead to the impact of ICD suppression.

PIAvh202 interacts with SAMS proteins of *Pe. litchii* in vivo and in vitro

To identify the host target of PIAvh202, total proteins were extracted from the *N. benthamiana* leaves transiently expressing GFP-tagged PIAvh202, and subject to immunoprecipitation (IP) for isolation of potential PIAvh202-interacting proteins. *N. benthamiana* expressing GFP served as a control. All purified proteins were analyzed utilizing liquid chromatography tandem-mass spectrometry (LC-MS/MS). Several potentially PIAvh202-associated proteins were detected, among which we identified an NbSAMS2-like protein (Supplemental Fig. S4A), and this protein was not detected in GFP-interacting proteins (Supplemental Table S2). We successfully cloned the NbSAMS2-like and its homologs (NbSAMS1 and NbSAMS3) based on NbSAMS sequences of NCBI (<https://www.ncbi.nlm.nih.gov/>) and Sol Genomics Network database (<https://solgenomics.net/>). GFP-NbSAMS1, GFP-NbSAMS2-like, GFP-NbSAMS3 or GFP was transiently co-expressed with PIAvh202-HA in *N. benthamiana* for Co-IP (Co-IP) assays. PIAvh202-HA was coimmunoprecipitated with GFP-NbSAMS1, GFP-NbSAMS2-like, and GFP-NbSAMS3 but not GFP (Supplemental Fig. S5A). This result suggests that PIAvh202 interacts with all 3 NbSAMSs in vivo. Besides, a glutathione S-transferase (GST) pull-down assay of coincubation between GST-tagged NbSAMSs protein and His-tagged PIAvh202 protein showed that His-tagged PIAvh202 could be pulled down by all 3 GST-tagged NbSAMSs but not GST control (Supplemental Fig. S5B), suggesting that PIAvh202 can interact with NbSAMS1, NbSAMS2-like, and NbSAMS3 in vitro.

To further validate the relationship between PIAvh202 and SAMS of litchi, 4 LcSAMS (*LcSAMS2*, *LcSAMS3*, *LcSAMS4*, and *LcSAMS5*) genes encoding the protein homologous to NbSAMS2-like were cloned from litchi cDNA and subsequently constructed into plasmid pCLuc, pBinGFP2 and pGEX-6P-1 for split luciferase complementation (SLC), Co-IP, and pull-down assays. Both SLC and Co-IP assays confirmed that PIAvh202 could interact with each of the 4 LcSAMSs in vivo (Fig. 6, A to C), and pull-down assays confirmed the interaction between PIAvh202 and all 4 LcSAMSs in vitro (Fig. 6D). Plant SAMSs can be classified as Type I and Type II, and Type I is 3 times more abundant than Type II (Sekula et al. 2020). Although both *LcSAMS2* and *LcSAMS3* belong to Type I group (Supplemental Fig. S4B), *LcSAMS3* was chosen for subsequent experiments because it showed higher similarity to NbSAMS2-like in protein sequence (Supplemental Fig. S4C).

SAMSs contribute to ICD and plant resistance against pathogens

To explore the role of SAMS in plant resistance, *LcSAMS3* was transiently expressed in *N. benthamiana* for challenging with

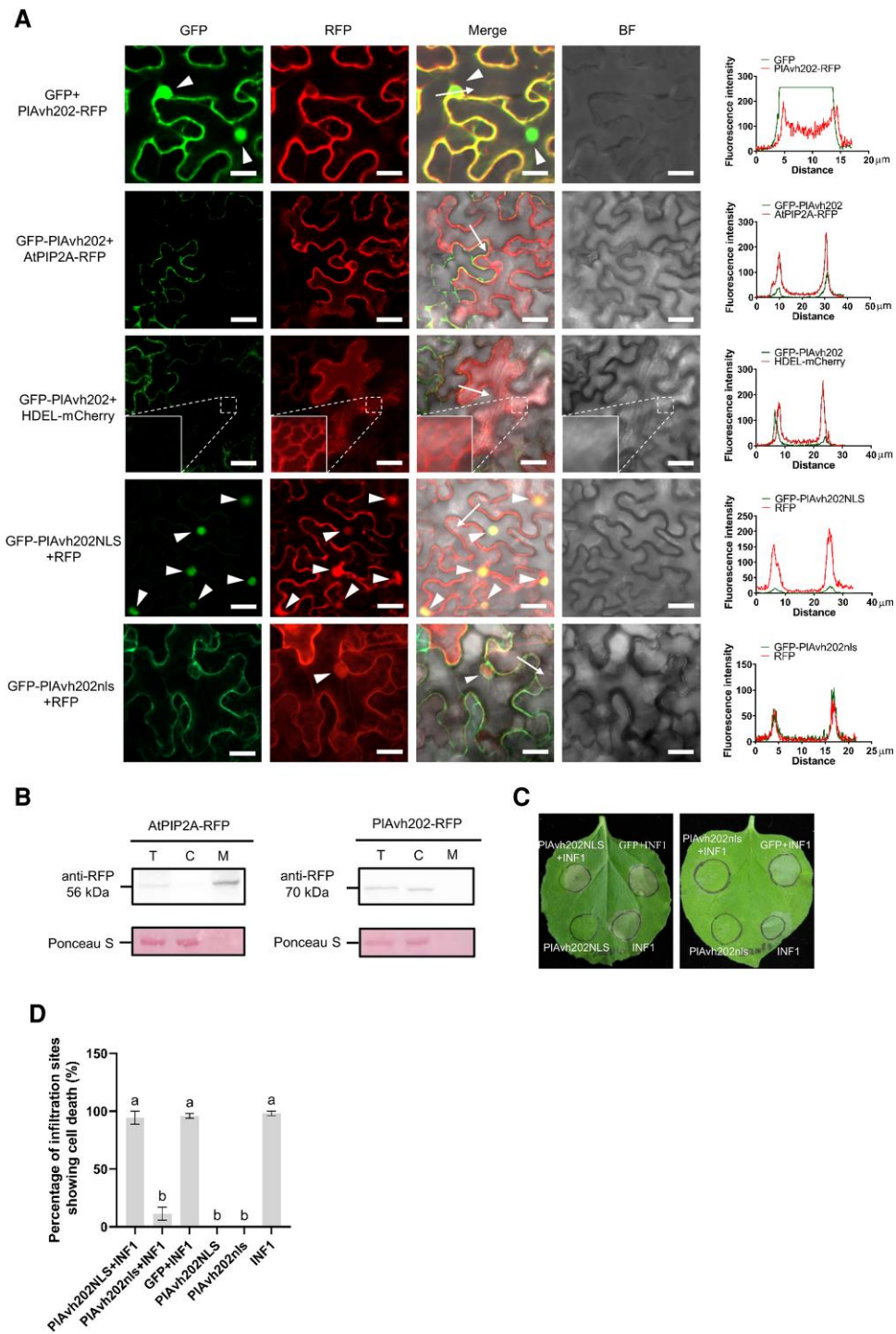


Figure 5. PIAvh202 mainly localizes to the cytoplasm. **A)** The localization of PIAvh202. GFP-PIAvh202, GFP-PIAvh202^{NLS}, GFP-PIAvh202^{nls}, or PIAvh202-RFP was individually coexpressed with AtPIP2A-RFP (a plasma membrane marker), HDEL-mCherry (an endoplasmic reticulum marker), RFP, or GFP in *N. benthamiana* leaf cells. Fluorescence was visualized by confocal microscopy at 36 hpi. Scale bars, 20 μm. A plot of the profile indicated by the white arrows shows GFP and RFP fluorescence signal at the region of interest; the white triangles indicate the cell nucleus. The right panel shows fluorescence intensity profiles of GFP and RFP. y-axis, GFP or RFP relative fluorescence intensity; x-axis, transect length (μm). **B)** Western blot analysis of proteins from *N. benthamiana* leaves transiently expressing PIAvh202-RFP or AtPIP2A-RFP. **C)** The nuclear localization of PIAvh202 led to the impact of ICD suppression. Agrobacterium carrying pBin::INF1-RFP was infiltrated into *N. benthamiana* leaves in which GFP-PIAvh202^{NLS}, GFP-PIAvh202^{nls}, or GFP was expressed. **D)** The statistical analysis for C). The cell death triggered by INF1 was scored from infiltration sites. Different letters represent significant differences using the 1-way ANOVA test followed by Tukey's honestly significant difference (HSD) test ($P < 0.05$). Data are the means \pm SD of 3 independent biological replicates ($n = 6$ leaves). T, total protein; C, cytosolic protein fraction; M, microsomal membrane protein fraction.

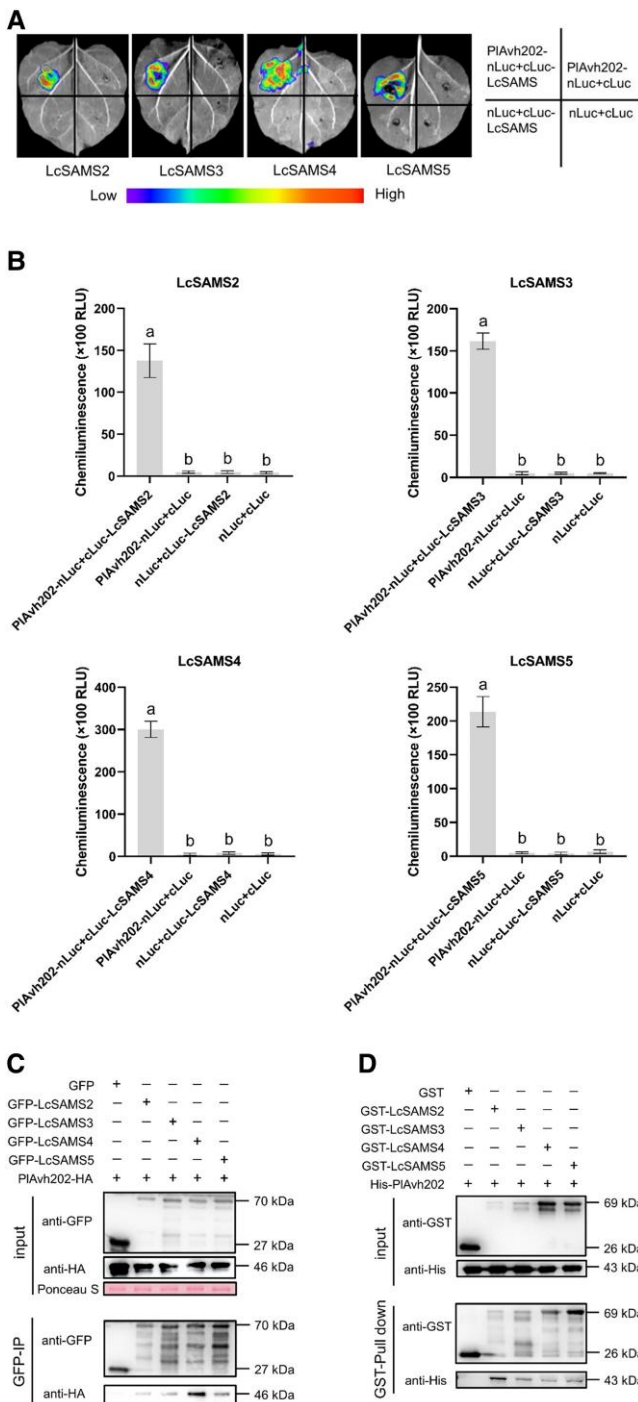


Figure 6. The interaction of PIAvh202 with LcSAMs in vivo and in vitro. **A**) SLC assays for the determination of interactions between PIAvh202 and LcSAMs. PIAvh202-nLuc was coexpressed with cLuc-LcSAMs2, cLuc-LcSAMs3, cLuc-LcSAMs4, or cLuc-LcSAMs5 in *N. benthamiana* leaves through agroinfiltration. Fluorescence signal intensity was recorded at 2 dpa. The image shown was representative of 3 biological replicates ($n = 5$). **B**) The measurement of LUC activity. The LUC activity represents the binding affinity between PIAvh202 and LcSAMs homologs. Different letters represent significant differences using the 1-way ANOVA test followed by Tukey's honestly significant difference (HSD) test ($P < 0.05$). Data are the means \pm SD of

Ph. capsici. Expression of LcSAMs3 led to smaller lesions and less biomass of *Ph. capsici* than that caused by RFP (Fig. 7A and Supplemental Fig. S6A), suggesting that LcSAMs3 positively regulates plant resistance. In addition, NbSAMs were silenced using virus-induced gene silencing (VIGS). As verified by RT-qPCR, the relative expression levels of 3 NbSAMs declined by 70% to 90% in comparison with GUS control (Fig. 7B). Although NbSAMs-silenced plants showed a slower growth than control (Supplemental Fig. S6B), they could be used for subsequent experiments at 30 days post-agroinfiltration (dpa). PIAvh202 or RFP was transiently expressed in the control or NbSAMs-silenced leaves, and *Ph. capsici* was inoculated in these leaves after 24 h. The lesion area and biomass of *Ph. capsici* on PIAvh202-expressing leaves were the same as that on RFP-expressing leaves when NbSAMs were silenced, whereas PIAvh202 still caused larger lesions and more biomass in the GUS control (Fig. 7, C and D). This result suggests that NbSAMs are essential for PIAvh202 to promote *Ph. capsici* infection. Besides, enhanced susceptibility to *Ph. capsici* was also observed in NbSAMs-silenced lines compared with GUS control (Fig. 7, C and D), highlighting the positive role of SAMs in regulating plant resistance to *Ph. capsici*. Moreover, a certain degree of ICD was diminished in NbSAMs-silenced *N. benthamiana* although the ICD was still visible, indicating that NbSAMs were involved in ICD (Fig. 7, C and E). In addition, RT-qPCR results showed that the expression levels of NbRbohA and NbRbohB in NbSAMs-silenced *N. benthamiana* declined by 55% and 72% compared with GUS control (Supplemental Fig. S6C), indicating that SAMs may contribute to ROS-based plant resistance and PCD. Taken together, these results support that PIAvh202 diminishes ICD and enhances plant susceptibility via NbSAMs.

Interaction with PIAvh202 leads to the degradation of LcSAMs

To determine which region of PIAvh202 is essential for interacting with LcSAMs3, GFP-tagged M1, M2, M3 and M4 were constructed to examine whether they could interact with LcSAMs3-HA using Co-IP. The results showed that LcSAMs3-HA was detected in the IP products of GFP-PIAvh202, GFP-PIAvh202M2, and GFP-PIAvh202M3, but not in that of GFP-PIAvh202M1, GFP-PIAvh202M4, and

Figure 6. (Continued)

3 independent biological replicates ($n = 8$). **C**) Coimmunoprecipitation of PIAvh202 by LcSAMs. PIAvh202-HA was coexpressed with GFP-LcSAMs2, GFP-LcSAMs3, GFP-LcSAMs4, or GFP-LcSAMs5 in *N. benthamiana* leaves, and total protein was extracted at 60 hpi. Protein complexes were pulled down utilizing GFP-Trap beads, and the captured proteins were detected by western blot using anti-HA antibody. Total protein was strained by Ponceau S. **D**) In vitro pull-down assays of PIAvh202 by LcSAMs. His-PIAvh202, GST-LcSAMs2, GST-LcSAMs3, GST-LcSAMs4, or GST-LcSAMs5 were expressed in *E. coli* and coincubated as indicated in the input. Coprecipitation of His-PIAvh202 with GST-binding proteins was detected by western blot using anti-His antibody. RLU, relative luminescence unit.

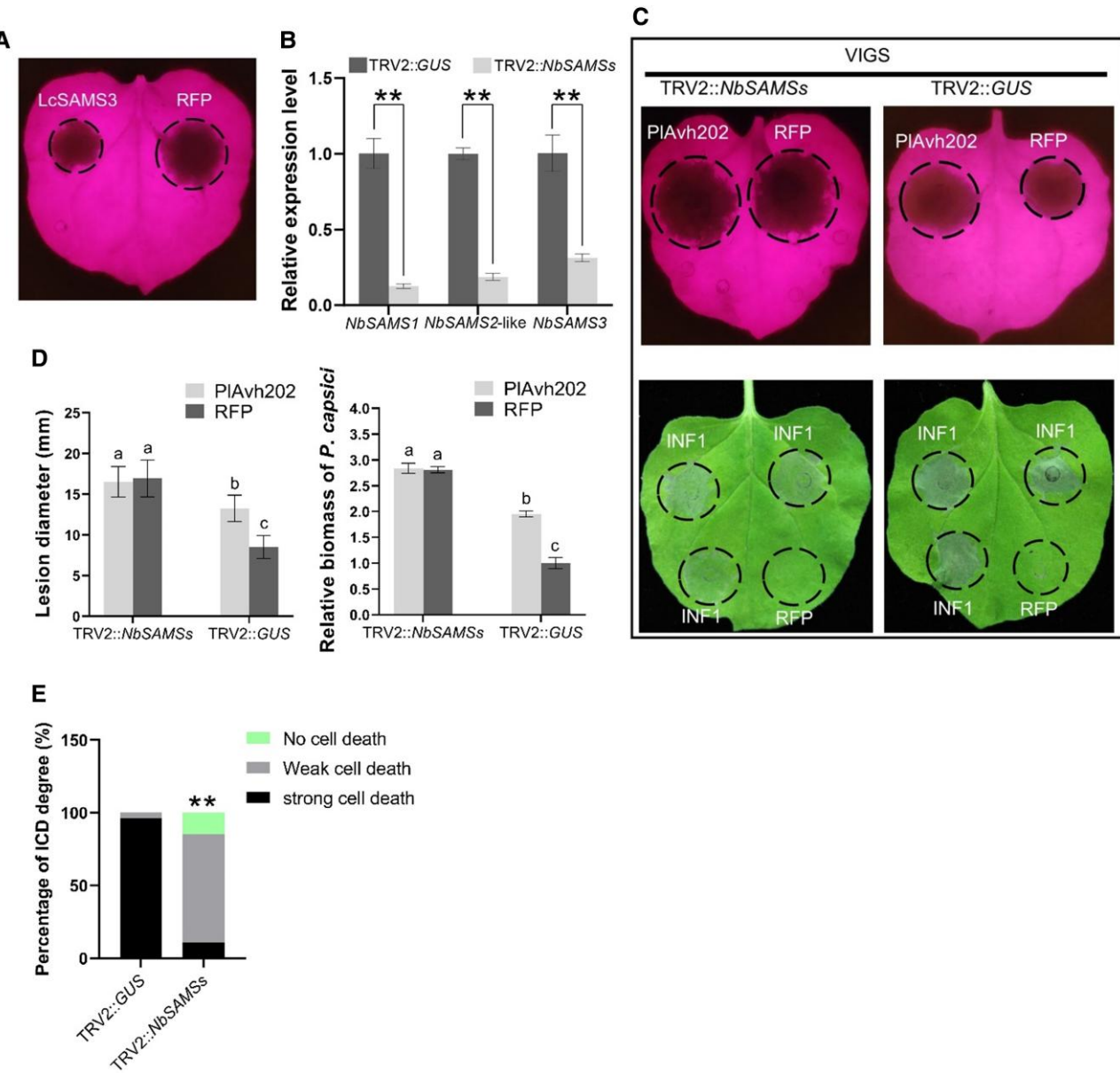


Figure 7. SAMSs positively regulate plant resistance. **A)** Transient expression of LcSAMS3 enhanced the resistance of *N. benthamiana* to *Ph. capsici*. *Ph. capsici* was inoculated in PIAvh202 or RFP-expressing *N. benthamiana* leaves, and photographs were taken under UV light at 36 hpi. **B)** Silencing efficiency of NbSAMSs. Relative expression levels of NbSAMS1, NbSAMS2-like, and NbSAMS3 were measured by RT-qPCR. Data are the means \pm SD of 3 independent biological replicates ($n = 3$ plants), asterisks represent significant differences ($**P < 0.01$, Student's *t* test). NbEF1 α was used as the internal reference. **C)** The silencing of NbSAMSs led to enhanced infection of *Ph. capsici* and diminished ICD. Top panel: *Ph. capsici* was inoculated in both sides of NbSAMSs-silenced *N. benthamiana* leaves expressing PIAvh202 and RFP, and photographs were taken at 36 hpi; bottom panel: INF1 or RFP was transiently expressed in NbSAMSs-silenced *N. benthamiana* leaves, and photographs were taken at 48 h post-agroinfiltration (hpa). TRV2::GUS was used as the control; black circles indicate lesion areas or cell death areas. **D)** Lesion diameter and biomass of *Ph. capsici* in NbSAMSs-silenced *N. benthamiana* leaves. Different letters represent significant differences using the 1-way ANOVA test followed by Tukey's honestly significant difference (HSD) test ($P < 0.05$). Data are the means \pm SD of 3 independent biological replicates ($n \geq 4$ leaves). **E)** The percentage of ICD degree. The cell death triggered by INF1 was scored from 18 infiltrated sites of SAMSs-silencing plants and GUS control. The degree of cell death was divided into 3 levels: no cell death, weak cell death, and strong cell death. Data are the means \pm SD of 3 independent biological replicates ($n = 3$ plants), asterisks represent significant differences ($**P < 0.01$, Wilcoxon rank-sum test).

GFP (Fig. 8A), suggesting that IR2 is required for the interaction between PIAvh202 and LcSAMS3. Interestingly, coexpression of PIAvh202 and LcSAMS3 appeared to reduce LcSAMS3 amounts in the Co-IP assay (Fig. 8A). To further

explore whether PIAvh202 alters LcSAMS3 stability, GFP, GFP-PIAvh202, and 4 mutants of GFP-PIAvh202 were coexpressed with LcSAMS3-HA in *N. benthamiana* to monitor the protein accumulation of LcSAMS3. According to the

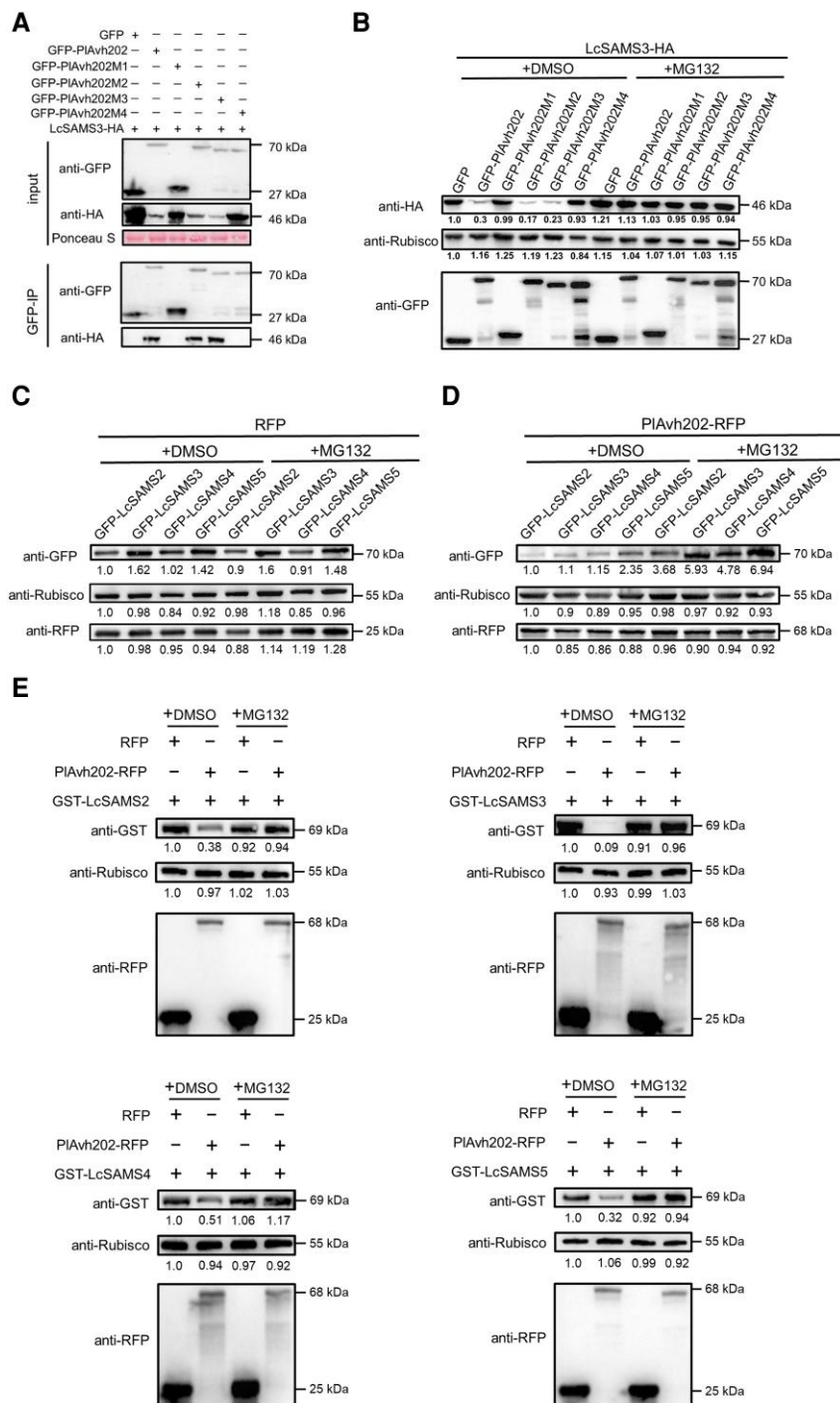


Figure 8. Association with PIAvh202 leads to 26S proteasome-mediated degradation of LcSAMSS in vivo and semi-in vitro. **A)** Coimmunoprecipitation of LcSAMSS by PIAvh202 and its mutants. LcSAMSS-HA was coexpressed with GFP-PIAvh202, GFP-PIAvh202M1, GFP-PIAvh202M2, GFP-PIAvh202M3, or GFP-PIAvh202M4 in *N. benthamiana* leaves, and total protein was extracted at 60 hpa. Protein complexes were pulled down utilizing GFP-Trap beads and the captured proteins were detected by western blot using anti-HA antibody. Total protein was strained by Ponceau S. **B)** Protein stability of LcSAMSS in the presence of PIAvh202 and its mutants. LcSAMSS-HA was coexpressed with GFP, GFP-PIAvh202, GFP-PIAvh202M1, GFP-PIAvh202M2, GFP-PIAvh202M3, or GFP-PIAvh202M4 in *N. benthamiana* leaves by agroinfiltration. These leaves were treated with dimethyl sulfoxide (0.5% DMSO, as a control) or MG132 (100 μ M) at 48 hpa and total protein was extracted at 60 hpa for western blotting. **C, D)** Protein stability of LcSAMSSs in vivo. The protein levels of GFP-LcSAMSSs were analyzed with anti-GFP in the presence of RFP **C)** or PIAvh202-RFP **D)** following DMSO or MG132 treatment. **E)** Protein stability of LcSAMSSs by semi-in vitro. The protein levels of purified GST-LcSAMSSs were analyzed with anti-GST in the presence of RFP or PIAvh202 following DMSO or MG132 treatment. The procedures of leaf infiltration and treatment with DMSO or MG132 were described above. In **B)** to **E)**, relative protein abundance was indicated by the numbers below the blot, anti-Rubisco was used as the loading control.

result of western blot, the accumulation of LcSAMS3-HA was reduced substantially in the presence of GFP-PIAvh202, GFP-PIAvh202M2 or GFP-PIAvh202M3 compared with GFP. However, the reduction of LcSAMS3 was not observed when LcSAMS3 was coexpressed with GFP-PIAvh202M1 or GFP-PIAvh202M4 (Fig. 8B). This result suggests that PIAvh202 interacts with LcSAMS3 via IR2 motif, which can destabilize LcSAMS3.

In order to test whether the destabilization of LcSAMS3 by PIAvh202 depends on 26S proteasome, the assay of LcSAMS3 stability was repeated in the presence of MG132, which is an inhibitor of the 26S proteasome (Zhang et al. 2015). As shown in Fig. 8B, the destabilization of LcSAMS3 by PIAvh202, PIAvh202M2, and PIAvh202M3 was inhibited by MG132 treatment. In addition, another 3 LcSAMSS (LcSAMS2, LcSAMS4, and LcSAMS5) were individually coexpressed with PIAvh202 in *N. benthamiana* to examine their protein stability. The result of western blot showed that PIAvh202 also destabilized these 3 LcSAMSS, and the destabilization could be inhibited by MG132 (Fig. 8, C and D and Supplemental Fig. S7). To further confirm the activity of PIAvh202 destabilizing LcSAMSS, we performed a semi-in vitro degradation assay. GST-tagged LcSAMS was incubated with protein crude extracts prepared from PIAvh202-RFP or RFP-expressing *N. benthamiana* leaves. The result showed that PIAvh202-RFP could promote the degradation of LcSAMSS compared with RFP control, and the degradation was inhibited by MG132 (Fig. 8E). Taken together, these findings support that PIAvh202 can destabilize LcSAMSS in an interaction-dependent manner. Because IR2 is required for PIAvh202 to suppress ICD (Fig. 4A) and destabilize SAMS (Fig. 8, A and B), and SAMS is involved in ICD (Fig. 7, C and E), we conclude that PIAvh202 targets and destabilizes plant SAMS to diminish ICD depending on IR2.

PIAvh202-mediated ET suppression enhances plant susceptibility

To examine whether the stability of LcSAMS3 can impact ET production, LcSAMS3 was coexpressed with GFP-PIAvh202, GFP-PIAvh202M2, GFP-PIAvh202M3, GFP-PIAvh202M4, and GFP control, respectively, in *N. benthamiana* to measure ET concentrations by gas chromatography. As shown in Fig. 9A, LcSAMS3 could induce ET production and the induction was significantly inhibited by GFP-PIAvh202, GFP-PIAvh202M2, GFP-PIAvh202M3 but not GFP-PIAvh202M4. Additionally, ET concentrations of MG132-treated plants were also measured. As expected, ET concentrations inhibited by GFP-PIAvh202, GFP-PIAvh202M2, and GFP-PIAvh202M3 could be restored to GFP level in the presence of MG132 (Fig. 9A). Moreover, RT-qPCR assays showed that coexpression of LcSAMS3 with PIAvh202 or its mutants could not affect the expression level of LcSAMS3 with or without MG132 (Supplemental Fig. S8A), suggesting that both PIAvh202 and MG132 were not able to inhibit LcSAMS3-induced ET production by down-regulating transcriptional levels of LcSAMS3. Given that PIAvh202,

GFP-PIAvh202M2, and GFP-PIAvh202M3 but not GFP-PIAvh202M4 could target and destabilize LcSAMS3 (Fig. 8, A and B), it is a conclusion that PIAvh202 can destabilize LcSAMS3 via 26S proteasome to inhibit LcSAMS3-induced ET production.

To confirm the relationship between reduced-ET production and PIAvh202 virulence, PIAvh202M3 or PIAvh202M4 was transiently expressed in *N. benthamiana* leaves to challenge with *Ph. capsici*. PIAvh202M3 was able to significantly promote *Ph. capsici* infection compared with RFP control, whereas PIAvh202M4 lost the ability to promote *Ph. capsici* infection (Fig. 9B and Supplemental Fig. S8, B and C), suggesting that ET suppression is required for PIAvh202 virulence. To further determine the function of ET in *Pe. litchii* infection, we inoculated *Pe. litchii* on litchi leaves which were pretreated with 50 μM AVG (aminoethoxyvinylglycine, an ethylene biosynthesis inhibitor), 100 μM ACC (a precursor of ethylene biosynthesis) or 0.02% Silwet L-77 buffer (as a control). Comparing with control, AVG-treated leaves displayed more severe symptoms of *Pe. litchii* infection, whereas ACC-treated leaves displayed less severe symptoms (Fig. 9C and Supplemental Fig. S8D), suggesting that ET production could promote litchi resistance to *Pe. litchii*. These results demonstrate that PIAvh202 promotes *Pe. litchii* infection by reducing ET production. Together, our findings suggest that PIAvh202 targets and promotes the degradation of LcSAMSS to reduce ET production, which could enhance plant susceptibility (Fig. 9D).

Discussion

Effectors secreted from bacterial, fungal and oomycetous pathogens interact with host plants to interfere with plant PTI and ETI; thus, they are usually used as molecular probes to reveal immune mechanisms in the pathogen-plant interaction (Toruño et al. 2016). In our study, we found that a *Pe. litchii* RXLR effector, PIAvh202, had a strong ability to suppress INF1-triggered immune responses, including ICD, the expression of immune maker genes, and ROS accumulation, suggesting that PIAvh202 can suppress INF1-triggered PTI. In addition, PIAvh202 can also suppress Avr3a/R3a triggered cell death, suggesting that PIAvh202 has a potential ability to suppress Avr3a/R3a-triggered ETI. Although PTI and ETI are activated by 2 distinct mechanisms, they can cause many overlapping immune responses, including calcium influx, phosphorylation or dephosphorylation of mitogen-activated protein kinase, ROS burst, and cell death (Adachi et al. 2015; Yuan et al. 2021a, b), suggestive of some intersectant points in these 2 pathways. In fact, recent researches support that PTI and ETI are not independent of each other. Instead, they can produce some similar defense-related secondary metabolites and phytohormones to jointly enhance plant immunity (Kadota et al. 2019; Yuan et al. 2021a, b; Zhai et al. 2022). This opinion is consistent with our finding that PIAvh202 can suppress both INF1-triggered PTI and Avr3a/R3a-triggered ETI. Moreover, the deletion of PIAvh202 impaired the virulence of *Pe. litchii*. These results

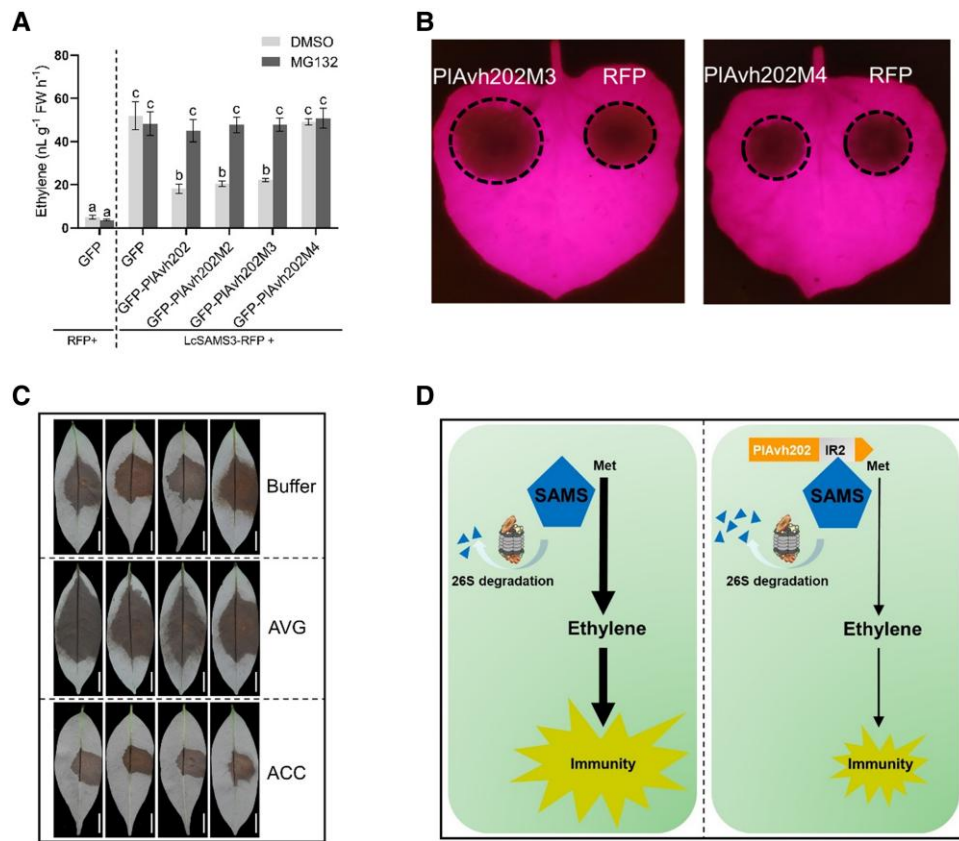


Figure 9. PIAvh202 enhances plant susceptibility by reducing LcSAMS-mediated ET production. **A)** PIAvh202, PIAvh202M2, and PIAvh202M3 inhibit ET production induced by LcSAMS3 in *N. benthamiana* leaves. These leaves that LcSAMS3 was coexpressed with PIAvh202, PIAvh202M2, PIAvh202M3 or PIAvh202M4 were treated with DMSO or MG132 and weighed at 24 hpa, and then the leaves were sealed in 10 mL glass vial to measure ET concentration using a gas chromatograph. Data are the means \pm SD of 3 independent biological replicates ($n \geq 6$ leaves), different letters represent significant differences using the 1-way ANOVA test followed by Tukey's honestly significant difference (HSD) test ($P < 0.05$). **B)** The reduced ET production led to enhanced susceptibility of plants to pathogens. RFP, PIAvh202M3, or PIAvh202M4 were transiently expressed in both sides of 1 leaf, and *Ph. capsici* was inoculated in these regions at 24 hpa. Photographs were taken under UV light at 36 hpi. **C)** ET promotes litchi resistance to *Pe. litchii*. Litchi leaves were sprayed with 100 μ M ACC, 50 μ M AVG or 0.02% Silwet L-77 (as a control), and were maintained at high humidity for 3 h. These leaves were then inoculated with 100 zoospores of *Pe. litchii* for infection analysis at 48 hpi. Bars = 1 cm. **D)** A schematic diagram illustrating that PIAvh202 suppresses ET-mediated plant immunity by destabilizing SAMS. PIAvh202 interacts with plant SAMS via the IR2 region, which leads to 26S proteasome-dependent degradation of SAMS. The destabilization of SAMS by PIAvh202 reduces ET production and ultimately results in the suppression of ET-mediated plant immunity.

demonstrate that PIAvh202 has an important virulence function via suppressing plant immunity. Therefore, PIAvh202 was used as a molecular probe to explore plant immune mechanisms.

PIAvh202 contains 2 IRs, among which the C-terminal motif IR2 is required to suppress ICD and promote *Ph. capsici* infection. This result was coincident with recent reports that the IRs of RXLR effectors PsAvh23 and PIAvh142 were required for their virulence function (Kong et al. 2017; Situ et al. 2020a). IR-containing proteins ubiquitously exist in all kingdoms of life and are responsible for binding diverse ligands, such as DNA, RNA, and proteins (Pawson and Nash 2003; Björklund et al. 2006). Our study showed that IR2 is essential for PIAvh202 to interact with its plant target proteins, SAMs, which is consistent with the protein-binding function of IRs. Previous studies showed that some viruses could

interfere with SAMs enzyme activity to create a more favorable environment for infection. For example, a Cotton Leaf Curl Multan virus (CLCuMuV) protein CLCuMuV C4 targets and inhibits NbSAMs2 enzyme activity to suppress both TGS (transcriptional gene silencing) and PTGS (post-transcriptional gene silencing)-based anti-viral defense in plants (Ismayil et al. 2018). Rice dwarf virus (RDV)-encoded Pns11 protein could enhance the enzymatic activity of OsSAMs1 to significantly increase rice ET production, resulting in higher susceptibility of rice to RDV (Zhao et al. 2017). In our study, PIAvh202 could promote the degradation of LcSAMs and reduce LcSAMs-catalyzed ET production, leading to diminished plant resistance to *Pe. litchii*. This action mode of PIAvh202 through 26S proteasome-mediated degradation of SAMs is distinct from that of the abovementioned virus proteins, which directly suppress or enhance SAMs enzymatic activity.

26S proteasome-mediated protein degradation usually depends on the ubiquitination of the target protein. For instance, the effector AvrPtoB contains a C-terminal E3 ubiquitin ligases domain and promotes the degradation of *Arabidopsis* CERK1 via the ubiquitin-26S proteasome system (Gimenez-Ibanez et al. 2009). However, PIAvh202 did not have a predicted ubiquitin ligases domain, suggesting that PIAvh202 may not directly ubiquitinate SAMS. Remarkably, a recent research showed that an effector could bridge target protein to 26S proteasome component RPN10 for 26S proteasome-mediated degradation in a ubiquitination-independent manner (Huang et al. 2021). It is possible that PIAvh202 may hijack the host protein to 26S proteasome for degradation without ubiquitination. It is of interest to explore whether ubiquitination is involved in PIAvh202-mediated SAMS degradation in the future.

In addition, our result that ET positively litchi resistance to *Pe. litchii* seems to be contrary to increased ET production resulting in the enhanced infection of RDV (Zhao et al. 2017). ET plays a complicated role in plant-pathogen interactions, as it can positively or negatively regulate disease resistance (Broekaert et al. 2006; van Loon et al. 2006). For example, while ethylene-insensitive mutants of *Nicotiana tabacum* showed lower susceptibilities to *Peronospora parasitica*, they showed higher susceptibilities to *Colletotrichum destructivum* and *Fusarium oxysporum* (Chen et al. 2003; Geraats et al. 2003). Generally, the precise role of ET in plant immune responses depends on the pathogen type and environmental conditions (Yang et al. 2013; Washington et al. 2016). Although ET is usually produced by plants to restrict the invasion of *Phytophthora* pathogens (Nunez-Pastrana et al. 2011; Sugano et al. 2013; Shen et al. 2016; Shibata et al. 2016), the function of ET in plant resistance to *Pe. litchii* has not been reported. Our results demonstrated that ET positively litchi resistance to *Pe. litchii*. Both flg22 and INF1 could induce ET production (Robert-Seilantian et al. 2011; Ohtsu et al. 2014), suggesting that ET contributes to plant PTI, which is consistent with our result that PIAvh202 inhibits INF1-induced PTI and ET production. Another RXLR effector, PsAvh238, could destabilize Type2 GmACS1 to reduce host plant ET production and facilitate *Ph. sojae* infection (Yang et al. 2019), suggesting that ET biosynthesis pathway is an important target attacked by oomycete effectors to suppress plant immune. This research is coincident with our results that PIAvh202 impairs ET biosynthesis by destabilizing SAMSs to suppress plant immunity.

Plant PCD can be triggered by the crosstalk between some proteases with ROS, phytohormone (ET), and calcium ions (Huysmans et al. 2017; Sychta et al. 2021). *NbRbohA* and *NbRbohB* of *N. benthamiana* are mainly responsible for ROS production to enhance PCD and resist oomycete pathogens (Yoshioka et al. 2003), and therefore are involved in INF1 or Avr3a/R3a-triggered PCD. Our results showed that ICD and expression of *NbRbohA* and *NbRbohB* were reduced in *NbSAMSs*-silenced plants, suggesting that *NbSAMSs* may contribute to ICD through Rbohs-mediated ROS production.

Moreover, a previous study showed that INF1 could induce ET production (Ohtsu et al. 2014), and elevated ET level was essential for ROS burst and PCD (Qin and Lan 2004; Liu et al. 2008; Yu et al. 2019). Given that SAMSs positively regulate ET production, it is a reasonable hypothesis that the destabilization of SAMSs by PIAvh202 reduces ET production, which compromises ROS accumulation and thus diminishes ICD. In addition, it remains unclear whether PIAvh202-mediated SAMSs destabilization is also involved in Avr3a/R3a-triggered PCD, which is worth further exploring in the future.

It is notable that the ICD in *NbSAMSs*-silenced plants is still visible although the degree of cell death is diminished compared with control, suggesting that PIAvh202 suppresses ICD may not only depend on SAMSs-mediated ET pathway, but there may be other plant target(s) of PIAvh202 to regulate ICD. Indeed, some effectors could associate with multiple plant targets to interfere with host immunity. For example, AvrB from *Ps. syringae* interacts with RAR1, RIN4, and RIPK to suppress flg22-induced PTI (Shang et al. 2006; Lee et al. 2015). Another effector AvrPtoB of *Ps. syringae* targets FLS2, BAK1, and ubiquitin to suppress plant immunity (Abramovitch et al. 2006; Goehre et al. 2008). Therefore, identifying more potential targets of PIAvh202, which are involved in ICD or Avr3a/R3a-triggered PCD, is important to explore PTI-ETI crosstalk.

In summary, our study demonstrates that an oomycete RXLR effector targets plant SAMSs to manipulate host ET-based immunity, revealing a mechanism of oomycetous pathogen-host plant interaction.

Materials and methods

Microbe and plant cultivation

Pe. litchii strain (SHS3) and *Ph. capsici* strain (PcLT263) were grown on CJA (carrot juice agar) medium in the dark at 25 °C. *Escherichia coli* strains DH5α, JM109, BL21 and *A. tumefaciens* (GV3101) were cultured on LB (Luria-Bertani) agar medium at 37 and 28 °C, respectively. *N. benthamiana* plants were grown in greenhouse at 25 °C with 16 h light and 8 h darkness. Litchi (*Litchi chinensis* Sonn.) leaves were obtained from the experimental orchard of South China Agricultural University in Guangzhou, China.

Plasmid construction

All primers in this study were listed in Supplemental Table S3. PIAvh202 and other *Pe. litchii* RXLR genes (without SP-encoding sequence) were amplified from the cDNA of *Pe. litchii*, *NbSAMS* and *LcSAMS* genes were amplified from the cDNA of *N. benthamiana* and *litchi*. These amplified fragments were digested with *Sma*I and cloned into pBinRFP and pBinGFP2 using ClonExpress II One Step Cloning Kit (Vazyme) for transient expression of *N. benthamiana*. In addition, the amplified fragments of PIAvh202 and SAMS were digested with *Bam*H I and *Eco*R I, respectively, and cloned into

pET32a and pGEX-6P-1 for protein expression and purification in *E. coli*. The vectors pYF2.3G-RibosgRNA and pBluescript II KS were used for the deletion of *PIAvh202* by CRISPR/Cas9-mediated genome editing technology (Fang et al. 2017; Situ et al. 2020a, b).

RT-qPCR assay

The total RNA of plant and microbe samples was extracted using an All-In-One DNA/RNA Mini-preps Kit (Bio Basic) following operation manual. gDNA buffer was added into total RNA to remove DNA impurity and then the purified RNA was used as a template to synthesized cDNA using a FastKing RT Kit (TIANGEN). The RT-qPCR assays were performed on qTOWER³ Real-Time PCR thermal cyclers (Analytik Jena) in 20 μ L reactions that contained 6.4 μ L deionized water, 10 μ L SYBR Premix ExTaq II (Takara), 0.4 μ m gene-specific primers and 20 ng cDNA. The specific reaction conditions are as follows: 95 °C for 2 min, 40 cycles at 95 °C for 30 s, and 60 °C for 30 s, followed by a dissociation progress, 95 °C for 15 s, 60 °C for 1 min, and 95 °C for 15 s.

Transient expression in *N. benthamiana* by *A. tumefaciens* infiltration

Recombinant plasmids were introduced into competent cells of *A. tumefaciens* strain GV3101 via heat shock. For infiltration, these transformed *A. tumefaciens* containing plant expression plasmids were incubated at 180 rpm, 28 °C for 36 h. The bacterial cells were collected and washed 3 times with 10 mM MgCl₂, 10 mM MES, pH 5.7, and 100 μ M acetosyringone at 4000 rpm for 4 min. Resuspended *A. tumefaciens* was infiltrated into 5 to 6 week-old *N. benthamiana* leaves by a 1 ml needless syringe at optical density (OD₆₀₀) of 0.4 to 0.6.

CRISPR/Cas9 mediated gene knockout of *PIAvh202*

The transformation of *Pe. litchii* was performed to delete *PIAvh202* as described previously (Fang et al. 2017; Situ et al. 2020a, b). In brief, the plasmid pYF2.3G-Ribo-sgRNA and pBluescript II KS of *PIAvh202* were constructed and co-transformed with pYF2-PsNLS-hSpCas9 into protoplasts of strain SHS3 mediated by polyethylene glycol. The transformants were screened on CJA plate supplemented with 50 μ g/mL G418. Then, these candidate transformants were subjected to extracted genomic DNA for PCR and sequencing.

For virulence analysis of transformants, 100 zoospores were inoculated on the tender leaves of litchi (Guwei) in the dark at 25 °C. Each transformant was inoculated at least 8 leaves. The lesion diameter was measured at 48 hpi.

Diaminobenzidine (DAB) staining

Effectors were transiently expressed in *N. benthamiana* and INF1 was expressed in the same site by agroinfiltration after 24 h. The ROS induced by INF1 accumulated for 36 h and then these leaves of *N. benthamiana* were collected to be stained with 1 mg/mL DAB for 8 h in the dark. The leaves

were boiled in absolute ethanol for 10 min to be for decolorization.

Ph. capsici inoculation assay

Two equal area grown mediums of *Ph. capsici* were inoculated on 2 sides of *N. benthamiana* leaves, respectively, in which *A. tumefaciens* was infiltrated 24 h ago. The leaves were photographed under UV light at 36 hpi and then collected to extract DNA for biomass analysis by qPCR.

Confocal microscopy

Fluorescent proteins were transiently expressed in *N. benthamiana* leaves using agroinfiltration, subcellular localizations were observed using an LSM 7810 (Carl Zeiss) laser scanning microscope with a \times 20 and \times 40 objective lens at 36 h post-infiltration. For GFP, the excitation and emission wavelength were 488 nm and 500 to 530 nm. For RFP, the excitation and emission wavelength were 561 nm and 588 to 641 nm.

Protein extraction and western blots

N. benthamiana leaves were collected at 36 h post-infiltration and ground in liquid nitrogen to be powder. About 100 mg plant powder and 0.1 mM protease inhibitor PMSF (no. ST507; Beyotime) were added into 600 μ L extraction buffer (no. P0013B; Beyotime) to release total protein. Besides, a protein extraction kit (P0033; Beyotime) was used for membrane and cytosol fractions (Yu et al. 2012). According to the product standard protocol, about 200 mg plant powder was dissolved into 1 mL buffer A, vortexed 30 s, and then centrifuged at 700 g for 10 min at 4 °C. Transferring supernatant to a new Eppendorf tube and centrifuged at 14,000 g for 30 min at 4 °C to precipitate membrane fraction, the supernatant (cytosol fraction) was collected in another new Eppendorf tube. The rest was centrifuged at 14,000 g for 10 s at 4 °C and removed supernatant as far as possible to reduce contamination of cytosol fractions. The precipitation was dissolved with 200 μ L buffer B, which was vortexed for 5 s and placed on ice for 10 min. Vortex and ice-bath was repeated twice. Then the sample was centrifuged at 14,000 g for 5 min at 4 °C, the supernatant was membrane fraction. The protein sample was boiled at 100 °C for 8 min with loading buffer and then separated on 12% (v/v) SDS-PAGE. After electrophoresis, the protein was treated as a standard protocol of western blot including membrane-transfer of polyvinylidene fluoride (PVDF), blocking with 5% (w/v) nonfat dry milk, overnight incubation of monoclonal antibodies (Chromotek) on ice at a 1:5000 dilution, PBST washing (3 times), incubation of goat anti-mouse horseradish peroxidase-conjugated secondary antibody (Dingguo) at a 1:5000 dilution and PBST washing (3 times). Finally, the proteins were visualized using ECL reagents in the imaging system (Bio-Rad).

Co-IP and LC-MS/MS analysis

Genes were constructed into pBinGFP2 for transient expression of *N. benthamiana*. At 36 hpa, the protein was extracted

from 1 g leaves using 2 mL extraction buffer (no. P0013; Beyotime) with 0.1 mM PMSF (no. ST507; Beyotime) and 0.1% (v/v) protease inhibitor cocktail (Sigma-Aldrich). The protein sample was centrifuged at 14,000 g for 10 min at 4 °C and then the supernatant was transferred in a new Eppendorf tube to incubate with 20 µL GFP-Trap-M beads (Chromotek) for 1 h at 4 °C. After that, the beads were collected by a magnetic grate of DynaMag™-2 (Invitrogen) and washed 4 times with wash buffer (10% (v/v) glycerol, 1 mM EDTA, 150 mM NaCl, 25 mM Tris-HCl (pH 7.5), 0.5% (v/v) Triton X-100% and 0.1% (v/v) protease inhibitor cocktail). For LC-MS/MS analysis, the beads were boiled with 40 µL SDT (4% (w/v) SDS, 100 mM Tris/HCl, 1 mM DTT (pH 7.6)) for 10 min and then sequenced by Beijing Genomics Institute (Shenzhen, China). For Co-IP, the beads were boiled with 40 µL protein loading buffer for 10 min, and then were used for western blotting.

GST pull-down

The plasmids pGEX-6P-1, pGEX-6P-1-SAMS and pET32a-PIAvh202 were expressed in *E. coli* strain BL21 to produce GST, GST-tagged SAMS and His-tagged PIAvh202 proteins in the condition of 18 °C, 180 rpm and 0.1 mM isopropyl-β-D-thiogalactopyranoside (IPTG) for 10 h. These bacteria were pelleted and lysed using a sonic dismembrator (WIGGENS) in the cold lysis buffer (1 × PBS (pH 7.4), 1% (v/v) Triton X-100% and 0.1% (v/v) protease inhibitor cocktail) to release soluble proteins. GST and GST-tagged SAMS were incubated with 40 µL GST magnetic beads (Thermo Fisher Scientific) for 1 h at 4 °C and then these beads were washed 3 times with lysis buffer. After that, the beads were incubated with His-tagged PIAvh202 1 h at 4 °C and then washed 3 times and boiled for 10 min. The denatured proteins were used for western blotting.

SLC assay

The coding sequence of PIAvh202 (without SP) or LcSAMSs was constructed into pCAMBIA1300-nLUC or pCAMBIA1300-cLUC, and then PIAvh202-nLuc was coexpressed with cLuc-LcSAMS in *N. benthamiana* via *A. tumefaciens*-mediated transient expression (described above). Three days post-agroinfiltration, 1 mM D-luciferin (Yeasen, China) was smeared onto infiltrated area. Luciferase signals were imaged using a low-light cooled charge-coupled device imaging system (NightSHADE LB 985 system, Berthold Technologies, Germany). For the quantitation of relative LUC activity, the leave discs were taken at 60 hpi and incubated with 1 mM D-luciferin in a 96-well plate for 10 min. The luminescence was detected using a microplate luminometer (Infinite 200 PRO, Tecan).

VIGS assays

The *A. tumefaciens* carrying TRV2::NbSAMS, TRV2::GUS or TRV1 was derived from preserved strains of our laboratory. Each of TRV2-harbored *A. tumefaciens* was mixed with TRV1 at a 1:1 ratio (each final OD₆₀₀ was 0.25), TRV2::GUS was a control. Then they were coinfiltrated into 2-week-old

N. benthamiana seedlings. After 3 weeks, the upper leaves were used for RT-qPCR to analyze silencing efficiency and subsequent experiments.

In vivo and semi-in vitro protein degradation

For in vivo assay of LcSAMS protein degradation by the 26S proteasome, PIAvh202 was coexpressed in *N. benthamiana* leaves with LcSAMS by *A. tumefaciens*-mediated transient expression. One hundred micromolar MG132 or 0.5% (v/v) DMSO was infiltrated into *N. benthamiana* leaves at 48 hpa and total protein was extracted for western blot at 60 hpa.

For semi-in vitro protein degradation assay, soluble crude extracts were prepared from *N. benthamiana* leaves using extraction buffer containing 10% (v/v) glycerol, 1 mM EDTA, 150 mM NaCl, 25 mM Tris-Cl (pH 7.5), 10 mM MgCl₂, 4 mM PMSF, 5 mM DTT, and 20 mM ATP as previously described with some modifications (Wang et al. 2009). The extracts were incubated with recombinant GST-LcSAMS protein at 23 °C for 90 min with or without 100 µM MG132. The reaction was stopped by adding 5 × protein loading sample buffer at 100 °C for 8 min for western blot analysis using anti-GST antibodies.

Ethylene quantification

N. benthamiana leaves treated by agroinfiltration 24 h ago were excised and weighed. Leaves were sealed in a 10 mL glass vial at 25 °C for 6 h. One microliter gas sample of head space was withdrawn and injected into the gas chromatography (Agilent 7890B) utilizing a gas-tight syringe to measure ethylene concentration. The column (Agilent, GS-Alumina; 50 m × 530 µm × 0 µm) was held at 50 °C for 3 min. The temperature of sample entry and hydrogen flame ionization detector (FID) was 200 °C and 300 °C, respectively. The peak area from gas chromatography was used to calculate ethylene concentration according to the standard curve.

Bioinformatic analysis

The sequence alignment was conducted using BioEdit7.0.5 software (<http://www.bioeditsoftware.informer.com>). Neighbor-Joining phylogenetic analysis was conducted using MEGA7.0 software (<https://www.megasoftware.net/>). The reliability of trees was estimated using 500 bootstrap iterations.

Statistical analysis

Statistical analysis was performed using Prism version 8 (GraphPad, La Jolla, CA, USA). Student's *t* test or 1-way ANOVA with Tukey's method was used to determine significance, and data are means ± SD of at least 3 independent experiments.

Accession numbers

Sequence data from this article can be found in the NCBI (<https://www.ncbi.nlm.nih.gov/>), SGN (<https://solgenomics.net/>), and SAP (<http://www.sapindaceae.com/>) databases. NCBI numbers: NbSAMS1 (KX452091) and NbSAMS3 (KX452093). SGN number: NbSAMS2-like (Niben101Scf01236g02016.1).

SAP numbers: LcSAMS2 (LITCHI014272.4), LcSAMS3 (LITCHI014272.3), LcSAMS4 (LITCHI024602.3), and LcSAMSS (LITCHI018653.1).

Acknowledgments

We thank Professor Brett Tyler (Oregon State University, United States) for CRISPR/Cas9 vectors and Professor Yuanchao Wang (Nanjing Agricultural University, China) for pBinGFP2 and pBinRFP vectors. We are grateful to Professor Yizhen Deng (South China Agricultural University, China) for critical reading, helpful discussion, and revision on the manuscript and to Professor Suomeng Dong (Nanjing Agricultural University, China) for the critical reading of the manuscript.

Author contributions

Z.J., G.K., and P.L. designed the research; P.L., W.L., X.Z., J.S., L.X., and P.X. performed the research; P.L., W.L., and X.Z. analyzed the data; P.L., G.K., and X.Z. wrote the paper; P.L., W.L., G.K., B.Y., and Z.J. discussed and commented on the manuscript; all authors read and approved the submitted version.

Supplemental data

The following materials are available in the online version of this article.

Supplemental Figure S1. Expression profile of PIAvh202.

Supplemental Figure S2. Knock-out of PIAvh202 by CRISPR/Cas9.

Supplemental Figure S3. Subcellular localization of PIAvh202 mutants.

Supplemental Figure S4. LC-MS/MS result and type of litchi SAMSS.

Supplemental Figure S5. PIAvh202 interacts with NbSAMS1, NbSAMS2-like, and NbSAMS3.

Supplemental Figure S6. LcSAMS3 promotes *Ph. capsici* infection and silencing NbSAMSS reduces the relative expression levels of *NbRbohA* and *NbRbohB*.

Supplemental Figure S7. PIAvh202 mediates LcSAMS protein degradation via 26S proteasome by *in vivo* assays.

Supplemental Figure S8. Ethylene (ET) contributes to the resistance of *N. benthamiana* and litchi.

Supplemental Table S1. RXLR effectors screening of ICD suppression.

Supplemental Table S2. PIAvh202-associating proteins detected by co-immunoprecipitation (Co-IP) followed by liquid chromatography-tandem mass spectrometry (LC-MS/MS).

Supplemental Table S3. Primers used in this study.

Funding information

This work was supported by the National Natural Science Foundation of China (U21A20220) and the earmarked fund for CARS-32.

Conflict of interest statement. The authors declare that they have no conflict of interest.

References

- Abramovitch RB, Janjusevic R, Stebbins CE, Martin GB.** Type III effector AvrPtoB requires intrinsic E3 ubiquitin ligase activity to suppress plant cell death and immunity. *Proc Natl Acad Sci USA*. 2006;103(8):2851–2856. <https://doi.org/10.1073/pnas.0507892103>
- Abramovitch RB, Kim YJ, Chen SR, Dickman MB, Martin GB.** *Pseudomonas* type III effector AvrPtoB induces plant disease susceptibility by inhibition of host programmed cell death. *EMBO J*. 2003;22(1):60–69. <https://doi.org/10.1093/emboj/cdg006>
- Adachi H, Nakano T, Miyagawa N, Ishihama N, Yoshioka M, Katou Y, Yaeno T, Shirasu K, Yoshioka H.** WRKY transcription factors phosphorylated by MAPK regulate a plant immune NADPH oxidase in *Nicotiana benthamiana*. *Plant Cell*. 2015;27(9):2645–2663. <https://doi.org/10.1105/tpc.15.00213>
- Anderson RG, Deb D, Fedkenheuer K, McDowell JM.** Recent progress in RXLR effector research. *Mol Plant Microbe Interact*. 2015;28(10): 1063–1072. <https://doi.org/10.1094/MPMI-01-15-0022-CR>
- Armstrong MR, Whisson SC, Pritchard L, Bos JIB, Venter E, Avrova AO, Rehmany AP, Bohme U, Brooks K, Cherevach I, et al.** An ancestral oomycete locus contains late blight avirulence gene *Avr3a*, encoding a protein that is recognized in the host cytoplasm. *Proc Natl Acad Sci USA*. 2005;102(21):7766–7771. <https://doi.org/10.1073/pnas.0500113102>
- Axtell MJ, Staskawicz BJ.** Initiation of RPS2-specified disease resistance in *Arabidopsis* is coupled to the AvrRpt2-directed elimination of RIN4. *Cell*. 2003;112(3):369–377. [https://doi.org/10.1016/S0092-8674\(03\)00036-9](https://doi.org/10.1016/S0092-8674(03)00036-9)
- Björklund AK, Ekman D, Elofsson A.** Expansion of protein domain repeats. *PLoS Comput Biol*. 2006;2(8):e114. <https://doi.org/10.1371/journal.pcbi.0020114>
- Broekaert WF, Delauré SL, De Bolle MF, Cammue BP.** The role of ethylene in host-pathogen interactions. *Annu Rev Phytopathol*. 2006;44(1):393–416. <https://doi.org/10.1146/annurev.phyto.44.070505.143440>
- Casteel CL, De Alwis M, Bak A, Dong HL, Whitham SA, Jander G.** Disruption of ethylene responses by *Turnip mosaic virus* mediates suppression of plant defense against the green peach aphid vector. *Plant Physiol*. 2015;169(1):209–218. <https://doi.org/10.1104/pp.15.00332>
- Chen N, Goodwin PH, Hsiang T.** The role of ethylene during the infection of *Nicotiana tabacum* by *Colletotrichum destructivum*. *J Exp Bot*. 2003;54(392):2449–2456. <https://doi.org/10.1093/jxb/erg289>
- DeFalco TA, Zipfel C.** Molecular mechanisms of early plant pattern-triggered immune signaling. *Mol Cell*. 2021;81(17):3449–3467. <https://doi.org/10.1016/j.molcel.2021.07.029>
- Ding P, Ding Y.** Stories of salicylic acid: a plant defense hormone. *Trends Plant Sci*. 2020;25(6):549–565. <https://doi.org/10.1016/j.tplants.2020.01.004>
- Dou D, Kale SD, Wang X, Chen Y, Wang Q, Wang X, Jiang RH, Arredondo FD, Anderson RG, Thakur PB, et al.** Conserved C-terminal motifs required for avirulence and suppression of cell death by *Phytophthora sojae* effector Avr1b. *Plant Cell*. 2008;20(4): 1118–1133. <https://doi.org/10.1105/tpc.107.057067>
- Du J, Verzaux E, Chaparro-Garcia A, Bijsterbosch G, Keizer LC, Zhou J, Liebrand TW, Xie C, Govers F, Robatzek S, et al.** Elicitin recognition confers enhanced resistance to *Phytophthora infestans* in potato. *Nat Plants*. 2015;1(4):15034. <https://doi.org/10.1038/nplants.2015.34>
- Dutra D, Agrawal N, Ghareeb H, Schirawski J.** Screening of secreted proteins of *Sporisorium reilianum* f. sp. *zeae* for cell death suppression in *Nicotiana benthamiana*. *Front Plant Sci*. 2020;11:95. <https://doi.org/10.3389/fpls.2020.00095>

- Fabro G, Steinbrenner J, Coates M, Ishaque N, Baxter L, Studholme DJ, Korner E, Allen RL, Piquerez SJ, Rougon-Cardoso A, et al.** Multiple candidate effectors from the oomycete pathogen *Hyaloperonospora Arabidopsis* suppress host plant immunity. *PLoS Pathog.* 2011;7(11):e1002348. <https://doi.org/10.1371/journal.ppat.1002348>.
- Fan XN, Che XR, Lai WZ, Wang SJ, Hu WT, Chen H, Zhao B, Tang M, Xie XA.** The auxin-inducible phosphate transporter AsPT5 mediates phosphate transport and is indispensable for arbuscule formation in Chinese milk vetch at moderately high phosphate supply. *Environ Microbiol.* 2020;22(6):2053–2079. <https://doi.org/10.1111/1462-2920.14952>
- Fang Y, Cui L, Gu B, Arredondo F, Tyler BM.** Efficient genome editing in the oomycete *Phytophthora sojae* using CRISPR/cas9. *Curr Protoc Microbiol.* 2017;44(1):21A.1.1–21A.1.26. <https://doi.org/10.1002/cmpc.25>
- Geraats BPJ, Bakker P, Lawrence CB, Achuo EA, Höfte M, van Loon LC.** Ethylene-insensitive tobacco shows differentially altered susceptibility to different pathogens. *Phytopathology.* 2003;93(7):813–821. <https://doi.org/10.1094/PHYTO.2003.93.7.813>
- Gimenez-Ibanez S, Hann DR, Ntoukakis V, Petutschnig E, Lipka V, Rathjen JP.** Avrptob targets the LysM receptor kinase CERK1 to promote bacterial virulence on plants. *Curr Biol.* 2009;19(5):423–429. <https://doi.org/10.1016/j.cub.2009.01.054>
- Goehre V, Spallek T, Haewecker H, Mersmann S, Mentzel T, Boller T, de Torres M, Mansfield JW, Robatzek S.** Plant pattern-recognition receptor FLS2 is directed for degradation by the bacterial ubiquitin ligase AvrPtoB. *Curr Biol.* 2008;18(23):1824–1832. <https://doi.org/10.1016/j.cub.2008.10.063>
- Gómez-Gómez L, Boller T.** FLS2: an LRR receptor-like kinase involved in the perception of the bacterial elicitor flagellin in *Arabidopsis*. *Mol Cell.* 2000;5(6):1003–1011. [https://doi.org/10.1016/S1097-2765\(00\)80265-8](https://doi.org/10.1016/S1097-2765(00)80265-8)
- Gonzalez E, Solano R, Rubio V, Leyva A, Paz-Ares J.** PHOSPHATE TRANSPORTER TRAFFIC FACILITATOR1 is a plant-specific SEC12-related protein that enables the endoplasmic reticulum exit of a high-affinity phosphate transporter in *Arabidopsis*. *Plant Cell.* 2005;17(12):3500–3512. <https://doi.org/10.1105/tpc.105.036640>
- Huang W, MacLean AM, Sugio A, Maqbool A, Busscher M, Cho ST, Kamoun S, Kuo CH, Immink RGH, Hogenhout SA.** Parasitic modulation of host development by ubiquitin-independent protein degradation. *Cell.* 2021;184(20):5201–5214.e12. <https://doi.org/10.1016/j.cell.2021.08.029>
- Huysmans M, Saul Lema A, Coll NS, Nowack MK.** Dying two deaths—programmed cell death regulation in development and disease. *Curr Opin Plant Biol.* 2017;35:37–44. <https://doi.org/10.1016/j.pbi.2016.11.005>
- Ismayil A, Haxim Y, Wang Y, Li H, Qian LC, Han T, Chen T, Jia Q, Yihao Liu A, Zhu S, et al.** Cotton Leaf Curl Multan virus C4 protein suppresses both transcriptional and post-transcriptional gene silencing by interacting with SAM synthetase. *PLoS Pathog.* 2018;14(8):e1007282. <https://doi.org/10.1371/journal.ppat.1007282>
- Jones JD, Dangl JL.** The plant immune system. *Nature.* 2006;444(7117):323–329. <https://doi.org/10.1038/nature05286>
- Jwa NS, Hwang BK.** Convergent evolution of pathogen effectors toward reactive oxygen species signaling networks in plants. *Front Plant Sci.* 2017;8:1687. <https://doi.org/10.3389/fpls.2017.01687>
- Kadota Y, Liebrand TWH, Goto Y, Sklenar J, Derbyshire P, Menke FLH, Torres MA, Molina A, Zipfel C, Coaker G, et al.** Quantitative phosphoproteomic analysis reveals common regulatory mechanisms between effector- and PAMP-triggered immunity in plants. *New Phytol.* 2019;221(4):2160–2175. <https://doi.org/10.1111/nph.15523>
- Kale SD, Gu B, Capelluto DG, Dou D, Feldman E, Rumore A, Arredondo FD, Hanlon R, Fudal I, Rouxel T, et al.** External lipid PI3P mediates entry of eukaryotic pathogen effectors into plant and animal host cells. *Cell.* 2010;142(2):284–295. <https://doi.org/10.1016/j.cell.2010.06.008>
- Kale SD, Tyler BM.** Entry of oomycete and fungal effectors into plant and animal host cells. *Cell Microbiol.* 2011;13(12):1839–1848. <https://doi.org/10.1111/j.1462-5822.2011.01659.x>
- Kamoun S, Furzer O, Jones JDG, Judelson HS, Ali GS, Dalio RJD, Roy SG, Schena L, Zambounis A, Panabieres F, et al.** The top 10 oomycete pathogens in molecular plant pathology. *Mol Plant Pathol.* 2015;16(4):413–434. <https://doi.org/10.1111/mpp.12190>
- Kong L, Qiu X, Kang J, Wang Y, Chen H, Huang J, Qiu M, Zhao Y, Kong G, Ma Z, et al.** A *Phytophthora* effector manipulates host histone acetylation and reprograms defense gene expression to promote infection. *Curr Biol.* 2017;27(7):981–991. <https://doi.org/10.1016/j.cub.2017.02.044>
- Lee D, Bourdais G, Yu G, Robatzek S, Coaker G.** Phosphorylation of the plant immune regulator RPM1-INTERACTING PROTEIN4 enhances plant plasma membrane H(+)-ATPase activity and inhibits flagellin-triggered immune responses in *Arabidopsis*. *Plant Cell.* 2015;27(7):2042–2056. <https://doi.org/10.1105/tpc.114.132308>
- Li Q, Ai G, Shen D, Zou F, Wang J, Bai T, Chen Y, Li S, Zhang M, Jing M, et al.** A *Phytophthora capsici* effector targets ACD11 binding partners that regulate ROS-mediated defense response in *Arabidopsis*. *Mol Plant.* 2019;12(4):565–581. <https://doi.org/10.1016/j.molp.2019.01.018>
- Liu H, Wang Y, Xu J, Su T, Liu G, Ren D.** Ethylene signaling is required for the acceleration of cell death induced by the activation of AtMEK5 in *Arabidopsis*. *Cell Res.* 2008;18(3):422–432. <https://doi.org/10.1038/cr.2008.29>
- Liu T, Ye W, Ru Y, Yang X, Gu B, Tao K, Lu S, Dong S, Zheng X, Shan W, et al.** Two host cytoplasmic effectors are required for pathogenesis of *Phytophthora sojae* by suppression of host defenses. *Plant Physiol.* 2011;155(1):490–501. <https://doi.org/10.1104/pp.110.166470>
- Liu Y, Lan X, Song S, Yin L, Dry IB, Qu J, Xiang J, Lu J.** In planta functional analysis and subcellular localization of the oomycete pathogen *Plasmopara viticola* candidate RXLR effector repertoire. *Front Plant Sci.* 2018;9:286. <https://doi.org/10.3389/fpls.2018.00286>
- Murphy F, He Q, Armstrong M, Giuliani LM, Boevink PC, Zhang W, Tian Z, Birch PRJ, Gilroy EM.** The potato MAP3K StVIK is required for the *Phytophthora infestans* RXLR effector Pi17316 to promote disease. *Plant Physiol.* 2018;177(1):398–410. <https://doi.org/10.1104/pp.18.00028>
- Naveed ZA, Wei XY, Chen JJ, Mubeen H, Ali GS.** The PTI to ETI continuum in *Phytophthora*-plant interactions. *Front Plant Sci.* 2020;11:593905. <https://doi.org/10.3389/fpls.2020.593905>
- Nunez-Pastrana R, Arcos-Ortega GF, Souza-Perera RA, Sanchez-Borges CA, Nakazawa-Uejii YE, Garcia-Villalobos FJ, Guzman-Antonio AA, Zuniga-Aguilar JJ.** Ethylene, but not salicylic acid or methyl jasmonate, induces a resistance response against *Phytophthora capsici* in habanero pepper. *Eur J Plant Pathol.* 2011;131(4):669–683. <https://doi.org/10.1007/s10658-011-9841-z>
- Ohtsu M, Shibata Y, Ojika M, Tamura K, Hara-Nishimura I, Mori H, Kawakita K, Takemoto D.** Nucleoporin 75 is involved in the ethylene-mediated production of phytoalexin for the resistance of *Nicotiana benthamiana* to *Phytophthora infestans*. *Mol Plant Microbe Interact.* 2014;27(12):1318–1330. <https://doi.org/10.1094/MPMI-06-14-0181-R>
- Park C, Lee HY, Yoon GM.** The regulation of ACC synthase protein turnover: a rapid route for modulating plant development and stress responses. *Curr Opin Plant Biol.* 2021;63:102046. <https://doi.org/10.1016/j.pbi.2021.102046>
- Pawson T, Nash P.** Assembly of cell regulatory systems through protein interaction domains. *Science.* 2003;300(5618):445–452. <https://doi.org/10.1126/science.1083653>
- Pieterse CMJ, Van der Does D, Zamioudis C, Leon-Reyes A, Van Wees SCM.** Hormonal modulation of plant immunity. *In R schekman, ed. Annu Rev Cell Dev Biol.* 2012;28(1):489–521. <https://doi.org/10.1146/annurev-cellbio-092910-154055>
- Qin WM, Lan WZ.** Fungal elicitor-induced cell death in *Taxus chinensis* suspension cells is mediated by ethylene and polyamines. *Plant Sci.* 2004;166(4):989–995. <https://doi.org/10.1016/j.plantsci.2003.12.013>
- Robert-Seilantian A, Grant M, Jones JD.** Hormone crosstalk in plant disease and defense: more than just jasmonate-salicylate antagonism.

- Annu Rev Phytopathol. 2011;49(1):317–343. <https://doi.org/10.1146/annurev-phyto-073009-114447>
- Sekula B, Ruszkowski M, Dauter Z.** S-adenosylmethionine synthases in plants: structural characterization of type I and II isoenzymes from *Arabidopsis thaliana* and *Medicago truncatula*. *Int J Biol Macromol.* 2020;151:554–565. <https://doi.org/10.1016/j.ijbiomac.2020.02.100>
- Shang Y, Li X, Cui H, He P, Thilmony R, Chintamanani S, Zwiesler-Vollick J, Gopalan S, Tang X, Zhou J-M.** RAR1, a central player in plant immunity, is targeted by *Pseudomonas syringae* effector AvrB. *Proc Natl Acad Sci USA.* 2006;103(50):19200–19205. <https://doi.org/10.1073/pnas.0607279103>
- Shen D, Chai C, Ma L, Zhang M, Dou D.** Comparative RNA-Seq analysis of *Nicotiana benthamiana* in response to *Phytophthora parasitica* infection. *Plant Growth Regul.* 2016;80(1):59–67. <https://doi.org/10.1007/s10725-016-0163-1>
- Shibata Y, Ojika M, Sugiyama A, Yazaki K, Jones DA, Kawakita K, Takemoto D.** The full-size ABCG transporters nb-ABCG1 and nb-ABCG2 function in pre-and postinvasion defense against *Phytophthora infestans* in *Nicotiana benthamiana*. *Plant Cell.* 2016;28(5):1163–1181. <https://doi.org/10.1105/tpc.15.00721>
- Situ J, Jiang L, Fan X, Yang W, Li W, Xi P, Deng Y, Kong G, Jiang Z.** An RXLR effector PIAvh142 from *Peronophythora litchii* triggers plant cell death and contributes to virulence. *Mol Plant Pathol.* 2020a;21(3):415–428. <https://doi.org/10.1111/mpp.12905>
- Situ J, Jiang L, Shaoy, Kong G, Xi P, Jiang Z.** Establishment of CRISPR/cas9 genome editing system in *Peronophythora litchii*. *J Fungal Res.* 2020b;18(3):181–188. <https://doi.org/10.13341/j.fjr.2020.1355>
- Sugano S, Sugimoto T, Takatsuji H, Jiang CJ.** Induction of resistance to *Phytophthora sojae* in soyabean (*Glycine max*) by salicylic acid and ethylene. *Plant Pathol.* 2013;62(5):1048–1056. <https://doi.org/10.1111/ppa.12011>
- Sychta K, Slomka A, Kuta E.** Insights into plant programmed cell death induced by heavy metals—discovering a *Terra Incognita*. *Cells.* 2021;10(1):65. <https://doi.org/10.3390/cells10010065>
- Teixeira RM, Ferreira MA, Raimundo GAS, Fontes EPB.** Geminiviral triggers and suppressors of plant antiviral immunity. *Microorganisms.* 2021;9(4):775. <https://doi.org/10.3390/microorganisms9040775>
- Toruno TY, Stergiopoulos I, Coaker G.** Plant-pathogen effectors: cellular probes interfering with plant defenses in spatial and temporal manners. *Annu Rev Phytopathol.* 2016;54(1):419–441. <https://doi.org/10.1146/annurev-phyto-080615-100204>
- Turnbull D, Yang L, Naqvi S, Breen S, Welsh L, Stephens J, Morris J, Boevink PC, Hedley PE, Zhan J, et al.** RXLR effector AVR2 up-regulates a brassinosteroid-responsive bHLH transcription factor to suppress immunity. *Plant Physiol.* 2017;174(1):356–369. <https://doi.org/10.1104/pp.16.01804>
- van Loon LC, Geraats BP, Linthorst HJ.** Ethylene as a modulator of disease resistance in plants. *Trends Plant Sci.* 2006;11(4):184–191. <https://doi.org/10.1016/j.tplants.2006.02.005>
- Wang Q, Han C, Ferreira AO, Yu X, Ye W, Tripathy S, Kale SD, Gu B, Sheng Y, Sui Y, et al.** Transcriptional programming and functional interactions within the *Phytophthora sojae* RXLR effector repertoire. *Plant Cell.* 2011;23(6):2064–2086. <https://doi.org/10.1105/tpc.111.086082>
- Wang F, Zhu DM, Huang X, Li S, Gong YN, Yao QF, Fu XD, Fan LM, Deng XW.** Biochemical insights on degradation of *Arabidopsis* DELLA proteins gained from a cell-free assay system. *Plant Cell.* 2009;21(8):2378–2390. <https://doi.org/10.1105/tpc.108.065433>
- Washington EJ, Mukhtar MS, Finkel OM, Wan L, Banfield MJ, Kieber JJ, Dangl JL.** *Pseudomonas syringae* type III effector HopAF1 suppresses plant immunity by targeting methionine recycling to block ethylene induction. *Proc Natl Acad Sci U S A.* 2016;113(25):E3577–E3586. <https://doi.org/10.1073/pnas.1606322113>
- Wawra S, Belmonte R, Löbach L, Saraiva M, Willemse A, van West P.** Secretion, delivery and function of oomycete effector proteins. *Curr Opin Microbiol.* 2012;15(6):685–691. <https://doi.org/10.1016/j.mib.2012.10.008>
- Whisson SC, Boevink PC, Moleleki L, Avrova AO, Morales JG, Gilroy EM, Armstrong MR, Grouffaud S, van West P, Chapman S, et al.** A translocation signal for delivery of oomycete effector proteins into host plant cells. *Nature.* 2007;450(7166):115–118. <https://doi.org/10.1038/nature06203>
- Yang B, Wang YY, Guo BD, Jing MF, Zhou H, Li YF, Wang HN, Huang J, Wang Y, Ye WW, et al.** The *Phytophthora sojae* RXLR effector Avh238 destabilizes soybean type2 GmACSS to suppress ethylene biosynthesis and promote infection. *New Phytol.* 2019;222(1):425–437. <https://doi.org/10.1111/nph.15581>
- Yang DL, Yang Y, He Z.** Roles of plant hormones and their interplay in rice immunity. *Mol Plant.* 2013;6(3):675–685. <https://doi.org/10.1093/mp/sst056>
- Ye W, Wang Y, Shen D, Li D, Pu T, Jiang Z, Zhang Z, Zheng X, Tyler BM, Wang Y.** Sequencing of the litchi downy blight pathogen reveals it is a *Phytophthora* species with downy mildew-like characteristics. *Mol Plant Microbe Interact.* 2016;29(7):573–583. <https://doi.org/10.1094/MPMI-03-16-0056-R>
- Yoshioka H, Numata N, Nakajima K, Katou S, Kawakita K, Rowland O, Jones JD, Doke N.** *Nicotiana benthamiana* gp91^{phox} homologs *NbrbohA* and *NbrbohB* participate in H₂O₂ accumulation and resistance to *Phytophthora infestans*. *Plant Cell.* 2003;15(3):706–718. <https://doi.org/10.1105/tpc.008680>
- Yu X, Tang J, Wang Q, Ye W, Tao K, Duan S, Lu C, Yang X, Dong S, Zheng X, et al.** The RxLR effector Avh241 from *Phytophthora sojae* requires plasma membrane localization to induce plant cell death. *New Phytol.* 2012;196(1):247–260. <https://doi.org/10.1111/j.1469-8137.2012.04241.x>
- Yu Y, Wang J, Li S, Kakan X, Zhou Y, Miao Y, Wang F, Qin H, Huang R.** Ascorbic acid integrates the antagonistic modulation of ethylene and abscisic acid in the accumulation of reactive oxygen species. *Plant Physiol.* 2019;179(4):1861–1875. <https://doi.org/10.1104/pp.18.01250>
- Yuan M, Jiang Z, Bi G, Nomura K, Liu M, Wang Y, Cai B, Zhou J-M, He SY, Xin X-F.** Pattern-recognition receptors are required for NLR-mediated plant immunity. *Nature.* 2021a;592(7852):105–109. <https://doi.org/10.1038/s41586-021-03316-6>
- Yuan M, Ngou BPM, Ding P, Xin XF.** PTI-ETI crosstalk: an integrative view of plant immunity. *Curr Opin Plant Biol.* 2021b;62:102030. <https://doi.org/10.1016/j.pbi.2021.102030>
- Zebell SG, Dong X.** Cell-cycle regulators and cell death in immunity. *Cell Host Microbe.* 2015;18(4):402–407. <https://doi.org/10.1016/j.chom.2015.10.001>
- Zhai K, Liang D, Li H, Jiao F, Yan B, Liu J, Lei Z, Huang L, Gong X, Wang X, et al.** NLRs guard metabolism to coordinate pattern- and effector-triggered immunity. *Nature.* 2022;601(7892):245–251. <https://doi.org/10.1038/s41586-021-04219-2>
- Zhang MX, Li Q, Liu TL, Liu L, Shen DY, Zhu Y, Liu PH, Zhou JM, Dou DL.** Two cytoplasmic effectors of *Phytophthora sojae* regulate plant cell death via interactions with plant catalases. *Plant Physiol.* 2015;167(1):164–175. <https://doi.org/10.1104/pp.114.252437>
- Zhao S, Hong W, Wu J, Wang Y, Ji S, Zhu S, Wei C, Zhang J, Li Y.** A viral protein promotes host SAMS1 activity and ethylene production for the benefit of virus infection. *Elife.* 2017;6:e27529. <https://doi.org/10.7554/elife.27529>
- Zipfel C, Kunze G, Chinchilla D, Caniard A, Jones JD, Boller T, Felix G.** Perception of the bacterial PAMP EF-Tu by the receptor EFR restricts *Agrobacterium*-mediated transformation. *Cell.* 2006;125(4):749–760. <https://doi.org/10.1016/j.cell.2006.03.037>